博士論文

Roles of RNaseT2 in the Regulation of Macrophage TLR Response to RNA Ligands

(RNA に対するマクロファージ TLR 応答の制御における RNaseT2 の役割)

劉　凱文

LIU KAIWEN

Contents

Abstract

Ribonuclease T2 (RNaseT2) is an RNase ubiquitously expressed in mammalian cells. It degrades RNAs in the endosomal compartments, while its roles in innate immune responses to RNA ligands have not been fully understood. Here, I show that RNaseT2 has positive and negative impacts on double-stranded RNA (dsRNA) sensor TLR3 and single-stranded RNA (ssRNA) sensor TLR7, respectively, in macrophages. RNaseT2 and RNase4, a member of RNase A family, were highly expressed in macrophages. Treatments with dsRNA or Type I interferon (IFN) upregulated RNaseT2 expression. RNaseT2-deficiency in macrophages led to upregulated TLR3 responses and impaired TLR7 responses. In mechanism, RNaseT2 degraded transfer RNA, dsRNA and TLR3 ligand poly(I:C) *in vitro*, and its mutants showed a positive correlation between RNase activity and the rescue of altered TLR3 and TLR7 responses. H122A and C118R mutation in RNaseT2 impaired RNase activity and the rescue of altered TLR3 and TLR7 responses. RNaseT2 showed broad distribution from early endosomes to lysosomes, where TLR3 and TLR7 are localized. RNaseT2 was also colocalized with the dsRNA poly(I:C). These results suggest that RNaseT2-dependent RNA degradation in endosomes or lysosomes negatively and positively regulates TLR3 and TLR7 responses, respectively, in macrophages.

Keywords: RNaseT2, TLR3, TLR7, innate immune

Introduction

Innate immunity and adaptive immunity

Immunity refers to the ability of organisms to recognize or distinguish pathogens and defend organisms against them. Immunity exists in a wide range of organisms from bacteria to mammals. Bacteria express enzymes to recognize and cleave the viral genome to suppress infection, while mammals have a complex immune system detecting infections of pathogens, interrupting pathogen activities, and wiping them out. The mammalian immune system consists of varieties of immune cells and molecules to contain pathogens.[1]

There are two types of immunity in mammals - innate immunity and adaptive immunity. Innate immunity refers to the immunity that works on most or at least a group of pathogens.[2,3] For example, skin is a barrier preventing most of the invading pathogens. There are other mechanisms in innate immunity, including the pattern receptors that recognize the typical molecular pattern from a group of pathogens and induce subsequent immune responses. Macrophages and dendritic cells (DCs), except for their antigen-presenting roles, are usually studied in the innate immune system.[2,4,5] The adaptive immunity, meanwhile, is like more "personalized" for each specific pathogen. It utilizes T lymphocytes and B lymphocytes specific to the pathogen to contain it invading or infecting. When an antigen is recognized and presented to the adaptive immune system, the lymphocytes specific to the antigen proliferate and differentiate to respond to it, by inducing cell death of the infected cells with T cells and producing antigen-specific antibodies with B cells. At the same time, memory T cells and memory B cells that memorize the antigen are also differentiated. Hence, with memory cells, the adaptive immune system is able mount quicker and stronger immune responses, when the same antigen is detected for a second time. Vaccines utilize this feature of adaptive immunity to

protect individuals from infection or suffering severe symptoms.[1,4]

Compared to innate immunity, adaptive immunity can respond specifically to a proper antigen and is still protective after the infection. Though, it usually takes time to mount the response for the first infection. The innate immunity, on the other hand, offers immediate response to pathogens and can induce adaptive immune response, by recruiting immune cells through producing chemokines and presenting antigens to lymphocytes. The two immune system work together to protect individuals from pathogens, as well as tumor cells, as tumor cells are also regarded as non-self.[1-3] However, immune response to self-derived antigens can lead to autoinflammation or autoimmune disorders.[6-8]

Toll-like receptors

In innate immunity, the membrane-spanning receptors, Toll-like receptors (TLRs), play essential roles by recognizing varieties of pathogen associated molecular patterns (PAMPs) or damage associated molecular patterns (DAMPs) and then inducing immune responses through the activation of downstream pathways.[5,8,9] These receptors are usually expressed in macrophages, dendritic cells and some even in neurons or epithelial cells.[5,10,11]

The name of the receptors, Toll-like, comes from the *Toll* gene identified from *Drosophila melanogaster*, which act as a receptor essential for the immune responses to fungal infections in *Drosophila.*[12] Mammalian homologues of the *Toll* gene were then discovered and named after it.[13] By present, 14 distinct mammalian TLRs have been identified in the family. There are 10 TLRs, TLR 1-10, identified in human. In mouse, TLR 1-9 and TLR11, TLR12 and TLR13 are identified, while TLR8 is not functional.[2,3,5,8]

TLRs are transmembrane molecules and function as dimers. Each TLR molecule holds one transmembrane helix domain. The N-terminal leucin-rich repeats (LRRs), acting as ligand-binding domain, is on the outer side of the cell membrane or the inner side of endosome or lysosome compartments, where the PAMPs and DAMPs are usually

localized.[2,8,14] The cytoplasmic C-terminal Toll/interleukin-1 receptor (TIR) homology domain functions as the trigger to the signaling cascade leading to immune responses through proper adaptors. When ligand binds to TLR, which changes the structure of dimer, the two TIR domains become closer to each other and thus activate the signaling pathway through the adaptors.[9,10,15,16] The heterodimers TLR1/TLR2 and TLR2/TLR6 recognize lipopeptide from bacteria, while homodimer of TLR5 is the sensor to flagellin, which forms bacterial flagella. TLR4 is also a bacteria sensor whose ligand is usually lipopolysaccharide (LPS), or known as endotoxin, forming the outer membrane of gram-negative bacteria.[2,5,8] TLR4 activation requires MD-2 (also known as LY96) and CD14 for interaction with LPS.[17] All these dimers above are localized on the cell surface. The nucleic acid sensing TLRs, including TLR3, TLR7, TLR8, TLR9 and mouse TLR13 on the other hand, are found on both cell surface and endosome or lysosome compartments. These five TLRs are also functioning as homodimers. TLR9 is a single-stranded DNA (ssDNA) sensor, which mainly recognizes the unmethylated CpG DNA from bacteria or DNA viruses. The other four TLRs are RNA sensors. TLR3 recognizes double-stranded RNA (dsRNA) generated during the infection of viruses. TLR7 and TLR8 are single-stranded RNA (ssRNA) sensors, also playing roles in antiviral responses against RNA viruses.[5,8] Mouse TLR13 recognizes bacterial ribosomal RNA (rRNA) -derived ssRNA based on the sequence.[18] (Fig. 1)

Two distinct signaling pathway can be activated by TLRs to induce immune responses. Either of the pathway has its own specific adaptor (Fig. 2). One of the pathways is the MyD88-dependent pathway. All TLRs except TLR3 signal through this pathway, in which MyD88 acts as the adaptor protein and activates the transcription factor nuclear factor-kappa B (NF-κB). This pathway also signals through interleukin-1 receptor associated kinase (IRAK).[9] The other pathway is called the TIR-domain-containing adapter-inducing interferon-β (TRIF)-dependent pathway and triggered only by TLR3 and TLR4. The TRIF-dependent pathway also activates NF-κB, as well as interleukin regulatory factor 3

(IRF3).[19-21] Activation of these pathways results in the production of type I interferon (IFN), cytokines and chemokines to activate immune cells or recruit them to the infection site. Typical cytokines or chemokines that can be induced by the activation of TLRs are interleukine-12 p40 (IL-12p40), which is generally specific to TLR responses, and CCL5, a chemokine produced in varieties of immune responses.

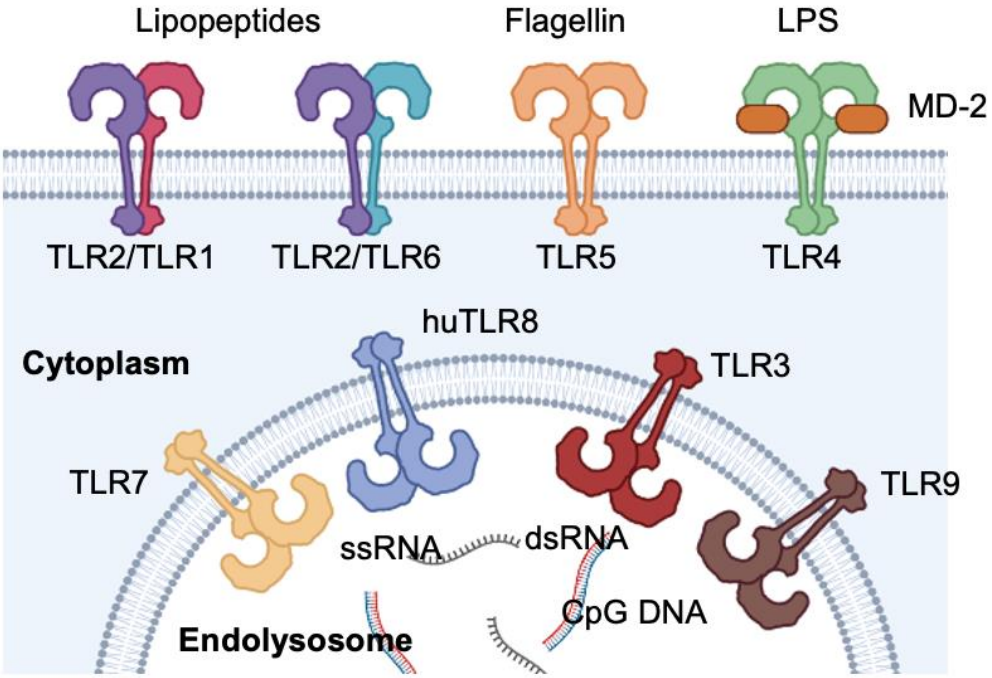

Figure 1. Localization and ligands of typical TLRs. TLR1, 2, 4, 5 and 6 are localized on cell surface, while TLR3, 7, 8 and 9 are localized on endolysosomes. TLR1/2 and TLR6/2 work as heterodimers and others function as homodimers. Ligands of TLRs are divided into lipids, proteins, and nucleic acids.

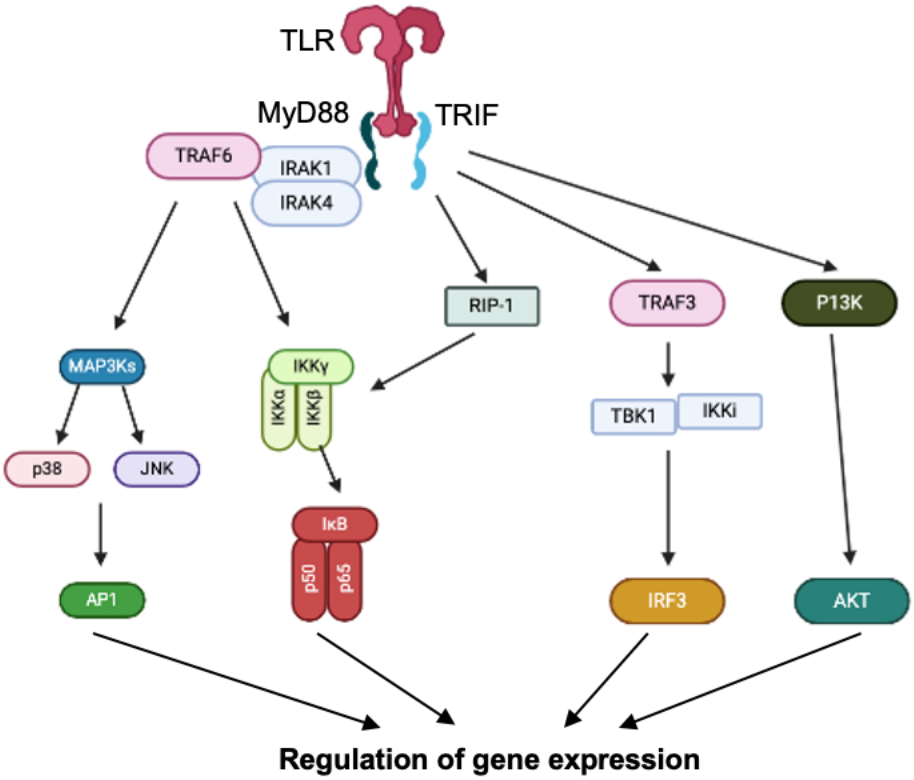

Figure 2. TLR signaling pathways. MyD88- and TRIF-dependent ways are shown. Both pathways lead to regulation of gene expression to induce immune responses.

Nucleic acid sensors in innate immunity

There are varieties of nucleic acid sensors working in innate immunity, including nucleic acid-sensing TLRs and other sensors. Despite the limited differences in the structure of nucleic acid between the host and pathogen, these sensors have their own way to distinguish between them. For example, nucleic acids from viruses are usually protected by viral membrane or proteins, and thereby difficult to be degraded in the extracellular space. Viral nucleic acids are usually transported into endosome or lysosome compartments and recognized by sensors localized there. Host derived nucleic acids are cleaved or degraded by deoxyribonucleases (DNases) and ribonucleases (RNases) to prevent activation of these sensors by self-derived molecules. Previous studies have shown the distribution of nucleic-sensing TLRs from endoplasmic reticulum (ER) to endolysosomes requires Unc93b1.

Unc93b1-deficiency impairs the immune responses of TLRs localized in the endosome or lysosome compartments.[22-24]

TLR9 is a ssDNA sensor, and localized on the membrane of endolysosomes. Just like other TLRs, it functions as homodimers. The ligand of TLR9 is unmethylated CpG DNA. As the CpG DNA in eukaryotic cells are usually methylated, it is a wise strategy to recognize unmethylated CpG DNA as the PAMP.[24,25] Stimulator of interferon genes (STING), also known as transmembrane protein 173 (Tmem173) is another important DNA sensor in innate immunity. STING is mainly localized in ER and activated by cyclic GMP-AMP (cGAMP) generated by an enzyme called cyclic GMP-AMP synthase (cGAS). Upon binding to double-stranded DNA (dsDNA), cGAS catalyzes GTP and ATP to form cGAMP. STING recognizes cGAMP and then induce immune responses through IRF3 and NF-κB transcription pathways. The cGAS-STING pathway is an important part of immune responses to DNA viruses and bacteria, that generating dsDNA in the cytoplasm during infections.[26,27]

As for RNA sensors among the TLR family, TLR3, TLR7 and human TLR8 are usually discussed. For a long time, both TLR7 and human TLR8 were regarded as ssRNA sensors, while recent reports have revealed their binding to the RNA degradation products, i.e., oligoribonucleotides (ORNs) and nucleosides, in the crystal structure of the two receptors. In detail, the two binding sites of TLR7 bind to guanosine and UUU, respectively and human TLR8 binds to uridine and UG in its two binding sites.[28,29] This means that the activation of TLR7 and human TLR8 requires a prior processing or degradation of RNA ligands into proper molecules by nucleic acid metabolic enzymes.[29-31] TLR7 and human TLR8 play roles in antiviral responses, as well as autoimmune disorders, including systemic lupus erythematosus (SLE) and rheumatic arthritis (RA).[6-8]

TLR3, the dsRNA sensor, unlike TLR7 or human TLR8, was reported to recognize dsRNA directly, and requires the dsRNA to be at least 40-50 base pairs (bp) in length.[32-34]

A zinc-finger protein named ZFYVE1 facilitates this ligand binding, and Mex3B acts as a coreceptor to present dsRNA to TLR3.[35-37] The signaling pathway of TLR3 is different from other TLRs, as it only signals through the TRIF-dependent pathway.[9] The ligand to TLR3, dsRNA is usually generated during RNA virus infection, and it has been reported that TLR3 is responsible for the immune responses to some RNA viruses, such as the Japanese encephalitis virus (JEV).[38] Surprisingly, there are also reports showing that TLR3 plays a vital role in the antiviral responses to some DNA viruses, such as herpes simplex virus (HSV) and Epstein-Barr virus (EBV).[39-41] Another special feature of TLR3 is its wide expression in a variety of cells including neurons and epithelial cells, in addition to commonly recognized immune cells. This also indicates the important role of TLR3 in immune responses of other systems like the nervous system.[11,40,42-44] About the immune responses related to TLR3, West Nile virus and HSV infections are frequently studied. Reports have shown that TLR3-deficiency, as well as deficiencies in molecules required for TLR3 responses or signaling, including Unc93b1, TRAF3, TBK1, IRF3 and STAT1, predisposes to herpes simplex encephalitis (HSE) during HSV infection.[43,45-47] Besides, the TLR3 response to self-derived ligands has been reported recently. Cells damages caused by ultraviolet (UV) or radiation lead to RNA release, and these RNA is likely to activate TLR3, inducing unnecessary inflammation.[48] Little is known, however, about the TLR3 ligands or TLR3-induced cytokine or IFN production during infections. Thus, it is important to understand the natural TLR3 ligand and mechanism of TLR3 response. TLR13 might be the least studied TLR family member, as it is not identified in human. Mouse TLR13 is a ssRNA sensor recognizing bacterial rRNA in a sequence specific way. It requires the ligand to be at least 12 bp in length and contain 5'-NNCGGAAAGNCN-3' sequence.[18]

Beside all the RNA-sensing TLRs in endolysosmes, retinoic acid-inducible gene-I (RIG-I) and melanoma differentiation associated protein 5 (MDA5) are dsRNA sensors localized

in cytoplasm.[49] They are the members of RIG-I like receptors. After binding to RNA, these receptors interact with the CARD domain of mitochondrial antiviral-signaling protein (MAVS) to active downstream signaling pathways to induce transcription of the genes encoding Type I IFNs and other immunoregulatory genes.[50]

Nucleases and immune responses

Nucleases are enzymes cleaving or degrading nucleic acids. According to the substrate, nucleases are generally divided into two groups - DNases and RNases.

DNases are enzymes digesting or degrading DNA and can be roughly divided into two groups - endodeoxyribonucleases, that cleave anywhere along the chain, and exodeoxyribonucleases, that cut only residues at the ends of DNA molecules. There are two main families of DNases in metazoans known as DNase I and DNase II. According to previous reports, DNases play essential roles in the response of DNA sensors. As for TLR9 responses, long ssDNA like CpG-A is not able to initiate the immune response through TLR9 directly. TLR9 activation requires the processing or cut of the long DNA ligand into short CpG DNA fragments by DNase II (Fig. 3 left side).[51] This also suggests that metabolic enzymes are required for immune responses by generating proper nucleic acid ligands to the receptors. Meanwhile, in the cGAS-STING responses to dsDNA in cytoplasm, as eukaryotic cells themselves can also generate DNA in cytoplasm, it is necessary to prevent the activation of the cGAS-STING pathway by these self-derived ligands. DNase II, again and Trex1 are vital in degrading these self-derived cytoplasmic DNA ligands to suppress hazardous activation of the cGAS-STING pathway (Fig. 3 right side).[52,53] It is reported that the *Dnase2a*$^{-/-}$ mice show embryonic death due to anemia as a consequence of constitutive production of IFN-β through cGAS-STING pathway.[54] Loss-of-function mutations of Trex1 in humans are reported to cause interferonopathy by constitutive activation of cGAS-STING pathway.[55] These studies have shown that DNase II

and Trex1 play roles in degradation of self-derived DNA, thus preventing the activation of cGAS-STING pathway by self-derived ligands, which shed light upon the functional relationship between DNA sensors and DNases.

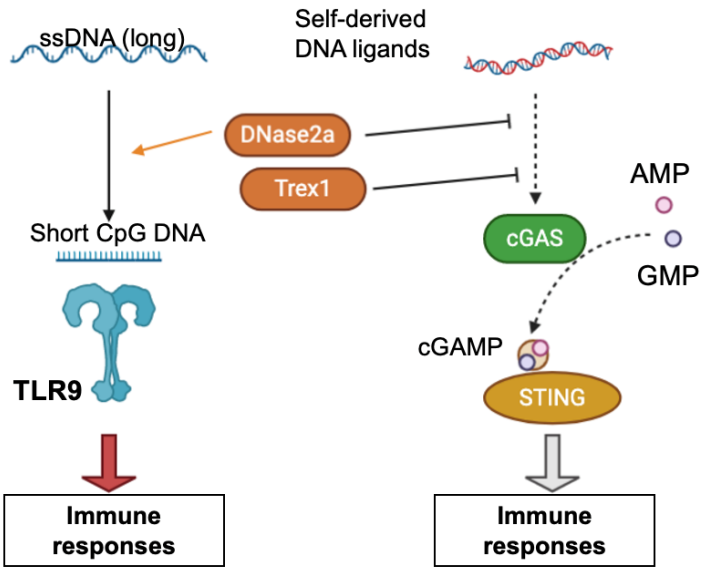

Figure 3. Regulation of immune sensors to DNA by DNases. TLR9 responses to ssDNA require the processing of long ssDNA into short fragments with CpG by DNase2a. DNase2a and Trex1 degrade self-derived DNA ligands to prevent activation of cGAS-STING pathway.

RNases are enzymes that cleave or degrade RNAs. There are numerous families of RNases identified by present from all the organisms, and many ribonucleases were found in mammals. Like DNases, RNases can also be roughly divided into two groups, the endoribonucleases recognizing proper sequence and cutting at a proper site, and the exoribonucleases digesting RNAs from 5'- or 3'-terminals. Among the families of RNases, RNaseA family is one of the best studied RNase family and widely used in researches. Its members are pyrimidine-specific endonucleases. In human, tens of RNaseA family members have been identified by present. In this family, RNA processing by RNase2 is required for the TLR8 responses.[56] RNase6 and RNase7 are reported to have antimicrobial function in human and/or murine urinary tract and skin.[57-59] RNaseT family is another family of

endoribonucleases. Unlike the RNaseA family, in mammals, only RNaseT2 is identified and reported to be functional.[60,61] RNaseT2 is a conserved protein in animals. Its homologs were found from yeast (*Saccharomyces cerevisiae*), named as RNY1, to human, encoded by *RNASET2* gene at 6q27, while no orthologs of it were found in a few species of animals, like rabbit (*Oryctolagus cuniculus*). In yeast, RNY1 cleaves transfer RNA (tRNA) and promotes cell death during oxidative stress in yeast.[62] Functionally, mammal RNaseT2 degrades rRNA and transfer tRNA in endosomes and mitochondrial RNA in the intermembrane space of mitochondria.[63–65] In studies on human RNaseT2, it is found that RNaseT2 is linked with suppression of tumorgenesis.[66,67] Loss-of-function mutations in RNaseT2, for example $RNASET2^{C184R}$, are linked with cystic leukoencephalopathy without megalencephaly in human.[68,69] Similar to human, RNaseT2-deficient rats show inflammations in the nervous system, suggesting the role of RNaseT2 in immune responses.[70] RNaseT2-deficient zebrafish also develop white matter lesions with lysosomal accumulation of rRNA in neurons.[63] Previous reports described similarities between cystic leukoencephalopathy without megalencephaly and Type I interferonopathy Aicardi-Goutières syndrome.[64,70] Taken together with the results that RNaseT2-deficient microglia contribute to leukoencephalopathy in zebrafish, macrophage activation due to RNaseT2-deficiency might contribute to the disease.[71] The role of RNaseT2, together with RNase2 in TLR8 responses has been studied recently. According to the two reports, RNaseT2 and RNase2 are required for TLR8 responses to ssRNA by degrading the ligand into uridine and ORN.[56,72] However, Impaired responses to ssRNA in RNaseT2-deficient macrophages might not be responsible for inflammatory responses in the brain of RNaseT2-deficient zebrafish or the nervous system of RNaseT2-deficient rat.[63,70,73] It is more likely that excessive activation of RNA sensors promotes disease progression in cystic leukoencephalopathy without megalencephaly.

In this study, I focused on the roles of RNases in the TLR responses to RNA ligands, as such regulations on TLR3 and TLR7 had not been reported like the human TLR8, TLR9 or cGAS/STING. I expected that through the study, one or several RNase(s) involved in these responses would be discovered, and that this would shed light upon the mechanisms of immune receptors recognizing nucleic acids. By examining RNase expression in macrophage cells with or without stimulation, I found high expressions of RNaseT2 and RNase4, while RNaseT2 was further induced after stimulation. RNaseT2-deficient cell line and bone marrow-derived cells exhibited upregulated responses to TLR3 ligand poly(I:C) and downregulated responses to TLR7 ligand polyU, without changes in the response to R848, the small chemical ligand to TLR7. To figure out the mechanism behind these regulations, the RNase activity of RNaseT2 was tested with both single-stranded and double-stranded RNAs, including the TLR3 ligands. RNaseT2 was localized in the endolysosomes and colocalized with dsRNA. These results suggest that RNaseT2 negatively regulates macrophage immune responses to dsRNA through degrading the ligands while this degradation is required for TLR7 responses to ssRNA.

Materials and Methods

Cell Lines

J774 mouse macrophage cell line and HEK293T cell line were cultured in complete RPMI 1640 medium (Nacalai Tesque) (10% FBS, 1 × Penicillin-Streptomycin-Glutamine (Gibco) and 50 μM β-mercaptoethanol (Nacalai Tesque)). PLAT-E cell line was cultured in complete DMEM (High Glucose) medium (Nacalai Tesque) (10% FBS, 1 × Penicillin-Streptomycin-Glutamine and 50 μM β-mercaptoethanol) with 1 μg/mL puromycin (InvivoGen) and 10 μg/mL blasticidin (InvivoGen). Ba/F3 cell line was cultured in complete RPMI 1640 medium with IL-3.

Guide RNA Sequences and Primers for Genotyping

All the primers and oligos were synthesized by FASMAC.

The sequences of sgRNAs, editing check primers and mouse genotyping primers used are as follows:

Rnaset2 gRNA1 (for cell line and mouse): CCGGGCTGGATCTCCGTGC,

Rnaset2 gRNA2 (only for mouse): GGAATTGAGGGCGTCTACCT,

Rnase4 gRNA: ACGGTTCCTTCGACAGCATG

Tlr3 gRNA: GTTCTTCACTTCGCAACGCA.

Rnaset2 gRNA1 check fw: CCTTATTGGGGGCCGTTACAGCGTGGG,

Rnaset2 gRNA1 check rv: CCCCTATGGCGCATATGTTGGAGGCAG.

Rnase4 gRNA check fw: GATCTACAGAGGACTCAGTC

Rnase4 gRNA check rv: AGTTCCCTGTCTCTCTGCAG

Rnaset2 WT fw: GACCTTTTGCGAGACATGAAGATCTACTGG,

Rnaset2 WT rv: TCCTACGATAAATCCTACCGGAGCTCATC;

Rnaset2 KO fw: AACCCCTTACTCTTCCGGATCTGGG,

Rnaset2 KO rv: GACACTGTAAAGTCTCTCATCATCCGC.

Antibodies

PE-conjugated mouse anti- TLR3 mAb (PaT3), PE-conjugated mouse anti- TLR7 mAb (A94B10) and APC-conjugated Amenian hamster anti-mouse CD11c mAb (N418) were purchased from BioLegend. Mouse anti-RNASET2 mAb (E-5) and Rabbit anti-Calnexin pAb (*#sc11397*) were purchased from Santa Cruz Biotechnology. PE-conjugated anti-mouse CD11b mAb (M1/70) was purchased from eBioscience. Rabbit anti-Actb mAb (SP124), Rabbit anti-Lamp1 pAb (*#ab24170*) and HRP goat anti-Mouse IgG antibody (*#ab97040*) were purchased from Abcam. Rabbit anti-EEA1 mAb (C45B10), Rabbit anti-Rab5 mAb (C8B1), Rabbit anti-Rab7a mAb (D95F2) and Rabbit anti-Golgin97 mAb (D8P2K) were purchased from Cell Signaling Technology. Rabbit anti-His-tag pAb (*#PM032*) was purchased from MBL. Alexa Flour 568 goat anti-Rabbit IgG (H+L) antibody (*#A11036*) and Alexa Flour 488 goat anti-Mouse IgG (H+L) antibody (*#A11029*) were purchased from Invitrogen. HRP-Labelled Protein A (*#NA9120*) was purchased from GE Healthcare.

Plasmid Construction

Original pMX4 and pLentiCRISPRv2 (pLCV2) plasmids were purchased from Addgene. The pLCV2 vectors (with puromycin or hygromycin resistant gene) are used for guide RNA and Cas9 expression, and the pMX4 vectors (with neomycin resistant gene) are used for over expression. Guide RNA sequences were designed with consensus sequences obtained from CCDS with CRIDPR direct, and DNA oligos with sticky end from the vector were synthesized. The DNA oligos were annealed and then linked into *BsmBI* (New England Biolabs) cut pLCV2 vectors using Quick Ligation Kit (New England Biolabs). Wild-type and mutated RNaseT2 genes with C-terminal FLAG-His tags were amplified by PCR from

mouse cDNA and cloned into *XhoI*/*NotI* (FastDigest, Thermo Fisher Scientific) cut pMX4 neomycin vectors using NEBuilder HiFi DNA Assembly Master Mix (New England Biolabs).

Real-time PCR Primers

Actb fw	GGATGACGATATCGCTGCGCTGG
Actb rv	GTGCCTAGGGCGGCCCACGATGG
Rnase1 fw	TCGTGCATGAGCCCTTGGCA
Rnase1 rv	GTAGTCACAGTTGGGATACT
Rnase4 fw	TCAGTCCTTGCTTCTGCTCTTGG
Rnase4 rv	CATTGCCACCTGTCACCTGAGGG
Rnase6 fw	CCATGCGCGGTGTCAACAATTAT
Rnase6 rv	CCGACCGTTCTTGCAGGTGATAT
Rnase9 fw	TTGGTCATCAAGTTCGCCTG
Rnase9 rv	TAATAAAGTCACGTACTTCT
Rnase10 fw	AGACTATCTAAAGCTGCTTA
Rnase10 rv	TAGGCCTAGCAACAGCAGCA
Rnase11 fw	TTGGACTGCTTCTTGCAAAG
Rnase11 rv	CCTCTAGAGTCTGTTTTGCAGCA
Rnase12 fw	AATGGTGGTTGTTTTCTTGC
Rnase12 rv	CCTCTGGAGAATCATGTAGTTGC
Rnase13 fw	GACAGGCATCACAATTCAGACGG
Rnase13 rv	TGAGGCCATTACAGTATCCGTGG
Rnaset2 fw	CCATCCATCAACTACTACCAGCT
Rnaset2 rv	TCTCTCCCTGTTCTGGCATAAGG
Ang fw	GGCCCGTTGTTCTTGATCTT,
Ang rv	TTTGGCTTGGCGTCATGGTG
Ang2 fw	CAGATACTGCGAAAGTATGA
Ang2 rv	ATTCTTAAATTTCGTCCATAAGG
Ang5 fw	CAGCCCAGGTTCTTTGTTGTTGG
Ang5 rv	CCTGTAGTTATCCTGAGCCAGAG
Ang6 fw	CCCAGGTTCCTTGATGTTGGTCT
Ang6 rv	CCTGTAGTTATCCTTAGCCAGAG
Ccl5 fw	CCCACGTCAAGGAGTATTTCTAC
Ccl5 rv	CCTTCGAGTGACAAACACGACTG
Ifnb1 fw	GACGAACATTCGGAAATGTCAGG
Ifnb1 rv	GATCTTGAAGTCCGCCCTGTAGG
Tlr3 fw	CATCTACAAAGTTGGGAACGGGG

Tlr3 rv	GTTCTTCACTTCGCAACGCAAGG
Tlr7 fw	CTAGAGTCTTTGGGTTTCGATGG
Tlr7 rv	CCCATGTGATCGTGGACTGCACA

Primers for Vector Construction

pMX4 Rnaset2 fw	AGCTAGTTAATTAAGGATCTCGAGATGGCGCCGGCG GAGGCTCGCGGCGCGCTCCCGGGCTGGATCTCCG TGCTGGGCTGGGG
Rnaset2 FLAG rv	CTTGTCATCGTCGTCCTTGTAGTCCTTGACGATCCT TCCTTCAATATGTTGGGTCTTTGTAGGTGG
FLAG His fw	ATTGAAGGAAGGATCGTCAAGGACTACAAGGACGA CGATGACAAGCACCATCACCATCACCATCACCATCA CCAT
FLAG His pMX4 rv	CGACCACTGTGCTGGCGGCCGCCTAATGGTGATG GTGATGGTGATGGTGATGGTGCTTGTCATCGT
H69A fw	AGACTCTCTGGATTACTGGACAATAGCCGGACTATGG CCCGATAGAGCAG
H69A rv	CTGCTCTATCGGGCCATAGTCCGGCTATTGTCCAGTA ATCCAGAGAGTCT
E118V fw	TCGCAGCCAATTCTGGAAACATGTGTGGGTTAAACAC GGCACCTGTGCTG
E118V rv	CAGCACAGGTGCCGTGTTTAACCCACACATGTTTCCA GAATTGGCTGCGA
H122A fw	TGGAAACATGAGTGGGTTAAAGCCGGCACCTGTGCT GCCCAGGTAGACGC
H122A rv	GCGTCTACCTGGGCAGCACAGGTGCCGGCTTTAACC CACTCATGTTTCCA
C188R fw	CTATGGTGTGGTGCCTAAAATCCAGCGCCTTATGCCA GAACAGGGAGAGA
C188R rv	TCTCTCCCTGTTCTGGCATAAGGCGCTGGATTTTAGG CACCACACCATAG

Virus Transfection and Transduction

HEK293T cells were planted in a collagen-coated 24-well plate at 3×10^5 per well. Lentivirus plasmid (pLCV2) was transfected using ViraPower Lentiviral Packaging Mix (Thermo Fisher Scientific) and PEI. Supernatant with virus was collected 48 hours later and applied to target cells. The cells were then cultured at 37 ºC and selection started at the following day. PLAT-E cells were planted in a collagen-coated 24-well plate at 2×10^5

per well. Retrovirus plasmid (pMX4) was transfected using FuGENE 6 Transfection Reagent (Promega). Supernatant with virus was collected 48 hours later and applied to target cells with DOTAP Liposomal Transfection Reagent (Sigma-Aldrich) at 2 μL/ 500 μL supernatant. The target cells were centrifuged at 2000 rpm/min for 1 hour and then cultured at 37 °C and selection started at the following day.

Mouse

C57BL/6 mice were purchased from Japan SLC Inc. The *Rnaset2a*$^{-/-}$ *Rnaset2b*$^{-/-}$ mouse was established in Laboratory of Reproductive Systems Biology, Center for Experimental Medicine and Systems Biology of IMSUT with CRISPR/Cas9 system. Two different guide RNAs targeting at both genes as well as the Cas9 protein were injected into zygotes and only the mouse with long deletions in both *Rnaset2a* and *Rnaset2b* genes was selected. In this manuscript, *Rnaset2a*$^{-/-}$ *Rnaset2b*$^{-/-}$ mice were described as *Rnaset2*$^{-/-}$ mice for simplicity.

Bone-Marrow Derived Macrophages, cDCs and pDCs

Bone marrow cells were harvested after mouse sacrificed. The red blood cells were then lysed with RBC Lysis Buffer (BioLegend) and the rest cells were planted in 10 cm dishes at 1×10^7 in 10 mL RPMI1640 (10% FBS, 1 × Penicillin-Streptomycin-Glutamine and 50 μM β-mercaptoethanol) per dish. The cells were cultured at 37 °C with 5 % CO_2 for a week and then harvested for further experiments. During the week, for BM-MCs, 10 ng/mL M-CSF was added, and 10 ng/mL GM-CSF for BM-cDCs. As for BM-pDCs, 10 ng/mL FLT3L was added, and the cells were sorted by $B220^+$ and $CD11c^+$ after 1 week.

HSV-1 Preparation

HSV-1 (F) were propagated in Vero cells. The virus was diluted 102-107-folds in

Medium 199 (Thermo Fisher Scientific) containing 1% FBS, and the Vero cells were infected in virus dilutions at 37 ° C. After 1 h, the culture medium was changed to Medium 199, containing 160 μg/ml human γ-globulin (Sigma Aldrich), and the cells were incubated at 37° C for 2 d. The number of plaques per well was counted to calculate the virus titer.

Influenza Virus Preparation

Influenza virus A/Puerto Rico/8/34 (H1N1) (PR8) was grown in the allantoic cavities of 10-day-old fertile chicken eggs at 35° C for 2 days. Virus was stored at −80° C and the viral titer was quantified in a standard plaque assay using MDCK cells.

Cell Stimulation and Examination of Cytokine Production by ELISA

Cells were planted on 96-well plates at 5×10^4 per well for J774 cells and 1×10^5 per well for bone-marrow derived cells. After adhering to the plates, the cells were treated with 200 U/mL IFN-β for 6 hours, if necessary, according to the experiment. Then, the cells were stimulated by proper ligands at proper concentrations. Ligands, including poly(I:C) HMW, polyU, R848, Lipid A and 2', 3' - cGAMP, were purchased from InvivoGen. 24 hours after the stimulation, culturing medium was collected, and the CCL5, TNF-α and IFN-α concentration was measured by Mouse CCL5/RANTES DuoSet ELISA Kit (R&D Systems), Mouse TNF alpha ELISA Ready-SET-Go! (eBioscience) and VariKine Mouse Interferon Alpha ELISA Kit (PBL assay science).

Realtime PCR

At least 5×10^5 cells were collected for each RNA sample. The RNA extraction was performed using RNeasy Mini Kit (QIAGEN). After extraction, the RNA was submitted to reverse transcription using ReverTra Ace qPCR RT Master Mix (TOYOBO) to obtain

cDNA. Finally, the cDNA was utilized for the real-time PCR performed with SYBR Green Realtime PCR Master Mix -Plus- (TOYOBO) and analyzed with StepOnePlus Realtime PCR System (Applied Biosystems) using ΔC_T or $\Delta\Delta C_T$ analysis. *Actb* was used as the endogenous reference.

Cell Staining and Flow Cytometry

Cells were stained and analyzed in FACS buffer (0.1% NaN_3, 2.5 % FBS in PBS). For permeabilized staining, Cytofix/Cytoperm Fixation/Permeabilization Kit (BD Biosciences) was applied to cells before staining the cells. Cells were analyzed with LSRFortessa X-20 Flow Cytometer (BD Biosciences) and the data was analyzed with FlowJo (v. 10).

RNaseT2 Protein Purification

Wild-type and mutated RNaseT2 with a C-terminal FLAG-His-tag were expressed in Ba/F3 cell line separately. Highly expressing clones were selected and cultured in large flasks. Cells were harvested and lysed with lysis buffer (1% Triton-X, 150 mM NaCl, 1 mM $CaCl_2$, 1 mM $MgCl_2$, 10% Glycerol and 20 mM Tris at pH 7.4 with cOmplete Protease Inhibitor Cocktail) on ice for 30 min. The lysate was centrifuged at 14,000 rpm for 20 min and the supernatant was collected for protein purification with ÄKTAprime plus (GE Healthcare) and His-Trap column (GE Healthcare). The purification was performed following the instructions attached with the His-Trap column. After purification, buffer change and protein concentration were performed with Amicon Ultra - 0.5 Centrifugal Filter Unit, 3 kDa (MERCK Millipore). Concentration of the RNaseT2 protein was measured with NanoDrop 2000c (Thermo Fisher Scientific) using protein assay according to previous reports.[60,68]

SDS-PAGE and Western Blotting

Samples were dissolved in SDS-PAGE sample buffer (50 mM Tris-HCl, 1% SDS, 10% Glycerol, 10% β-mercaptoethanol and 0.1% bromophenol blue) and incubated at 98 ºC for 10 min. Then, the samples were load to Extra PAGE One Precast Gel, 5-20 % (Nacalai Tesque), and electrophoresis was performed at 20 mA per gel for 80 min in SDS-PAGE buffer (25 mM Tris, 192 mM glycine, 0.1% SDS). The protein in the gel was transferred to an Immobilon-P PVDF Membrane (MERCK Millipore) at 125 V for 1 hour in transfer buffer (25 mM Tris, 20% methanol, 192 mM glycine). The membrane was blocked in Blocking One (Nacalai Tesque) for 20 min and the antibodies were applied to the membrane in Can Get Signal Immnunoreaction Enhancer Solution (TOYOBO). After application of antibodies and wash by TBS-Tween, Amersham ECL Select Western Blotting Detection Reagent (GE Healthcare) was applied to the membrane. Images were captured by ImageQuant LAS 500 (GE Healthcare).

RNA digestion with RNaseT2

Yeast transfer RNA, DynaMarker dsRNA Ladder Marker (BioDynamics Laboratory) or poly(I:C) was first diluted in reaction buffer (0.1 M NaAc, 0.1 M KCl, pH 5.0) to 200 ng/μL. 50 ng of purified RNaseT2 protein was added to 10 μL of the diluted RNA in PCR tubes. The tubes were incubated at 37 ºC for 1 hr. for the reaction and then at 95 ºC for 1 min to deactivate the protein. Then, transfer RNA was analyzed with MultiNA (SHIMADZU), and the two types of dsRNA were analyzed with 2% agarose gel stained by ethidium bromide (Nacalai Tesque). After analysis with agarose gel, the relative concentration of each band in the dsRNA marker was calculated by GelAnalyzer (ver. 19.1).

Confocal Microscopy

Cells were planted on a sterile collagen (Cellmatrix Type I-P, Nitta Gelatin)-coated micro cover glass (MATSUNAMI) in 12-well plate. After adhering, some samples were treated with 0.2 μg/mL Poly(I:C)-Rhodamine (InvivoGen). Then the cells were fixed with 4% PFA (Thermo Fisher Scientific) in PBS for 10 min, permeabilized with 0.2% saponin in PBS for 30 min and blocked with confocal microscopy blocking buffer (2.5% BSA, 0.01% NaN_3, 1 × PBS and 50% Blocking One) for 30 min. After washed with PBS, the cells were stained with primary antibodies in confocal microscopy blocking buffer at 37 °C for 1.5 hour and washed with PBS for 3 times. Then, the cells were stained with Alexa Fluor-conjugated secondary antibodies and DAPI at in confocal microscopy blocking buffer at 37 °C for 1.5 hour and washed with PBS for 3 times. Finally, the cover glass was mounted on a micro slide glass (MATSUNAMI) with PermaFluor mountant (Thermo Fisher Scientific). Image capturing and subsequent analyses were performed by ZEISS LSM 710 confocal microscope with ZEN software.

Separation of Cell Organelles by Density-Gradient Centrifugation

1 ~ 2 × 10^7 cells were harvested and homogenized in 450 μL homogenization buffer (50 mM HEPES, 78 mM KCl, 4 mM $MgCl_2$, 8.4 mM $CaCl_2$, 10 mM EGTA and 250 mM Sucrose with Halt Protease Inhibitor Cocktail) by passing through a 29-gauge needle util the cells show roughly 70 ~ 80% trypan blue positive. Then the mixture was centrifuged at 1,000 × g for 5 min and only supernatant was collected. 360 μL of each of the gradient solution (30%, 23%, 17%, 11% and 5% Opti-prep in working buffer (50 mM HEPES, 78 mM KCl, 4 mM $MgCl_2$, 8.4 mM $CaCl_2$ and 10 mM EGTA)) were layered in a centrifuge tube from the heaviest one to the lightest one and the collected supernatant was layered on the top. This gradient was centrifuged for 4 hr. at 130,000 × g at 4 °C with Rate 8 acceleration and free deceleration. After centrifugation, 11 fractions were collected every 185 μL from top to

bottom. These fractions were analyzed by immunoblotting.

Statistical Analysis

Data from triplicate samples were analyzed with Student's *t*-test. Differences among multiple groups were analyzed with one-way ANOVA. *P* values of < 0.05 were considered significant.

Results

RNase4 and RNaseT2 were highly expressed in macrophages

To study the possible roles of RNases in macrophage TLR responses to RNA ligands, the expression of mRNAs encoding members of the RNaseA and RNaseT families was first studied in the mouse macrophage cell line J774, and bone marrow derived macrophages (BM-MCs). Among these RNases investigated, RNase4, RNase6, RNaseT2 and Ang were expressed in both type of macrophages (Fig. 4a, 4b). Compared to other two molecules, the amount of mRNA encoding RNase4 and RNaseT2 was much higher. The expression of RNase4 and RNaseT2 in spleen macrophages was also studied. The two RNases were comparably expressed in $F4/80^{+}$ $CD11b^{+}$ red pulp macrophages, whereas RNase4 expression was lower than RNaseT2 in $F4/80^{-}$ $CD11b^{+}$ macrophages (Fig. 4c).

RNase expression in bone marrow derived plasmacytoid dendritic cells (BM-pDCs) and bone marrow derived conventional dendritic cells (BM-cDCs) was also examined in mRNA level. In BM-pDCs, RNaseT2 and RNase6, instead of RNase4 in RNaseA family, was highly expressed, while in BM-cDCs, RNaseT2 was highly expressed, with a relatively lower RNase4 expression compared to macrophages (Fig. 4d, 4e).

RNaseT2 expression increased upon activation in macrophages

The mRNA levels when cells were stimulated with ligands were also studied. J774 cells and BM-MCs were treated with TLR3 ligand poly(I:C), TLR7 ligand polyU, TLR9 ligand CpG-B, TLR13 ligand Sa19 or TLR4/MD-2 ligand Lipid A for 24 hours, and the mRNA induction of the highly expressed RNases, i.e., RNase4 and RNaseT2, compared to cells left unstimulated, was examined. After stimulation, RNase4 mRNA transcription was downregulated in response to all the stimulants in both types of cells. For RNaseT2,

poly(I:C) and Lipid A stimulation led to an upregulation in its mRNA transcription (Fig. 5a, 5b). As these ligands also lead to production of Type I IFN, the mRNA level of the two RNases in BM-MCs after IFN-β treatment was also examined. The result showed as early as 3 hours from treatment, the mRNA encoding RNaseT2 was significantly upregulated (Fig. 5c). Like in ligand treatment, mRNA encoding RNase4 was downregulated (Fig. 5d). As RNaseT2 can be induced after ligand stimulation or Type I IFN treatment, it is likely that RNaseT2 play roles in some immune responses. Here, I focused on RNaseT2 for further study.

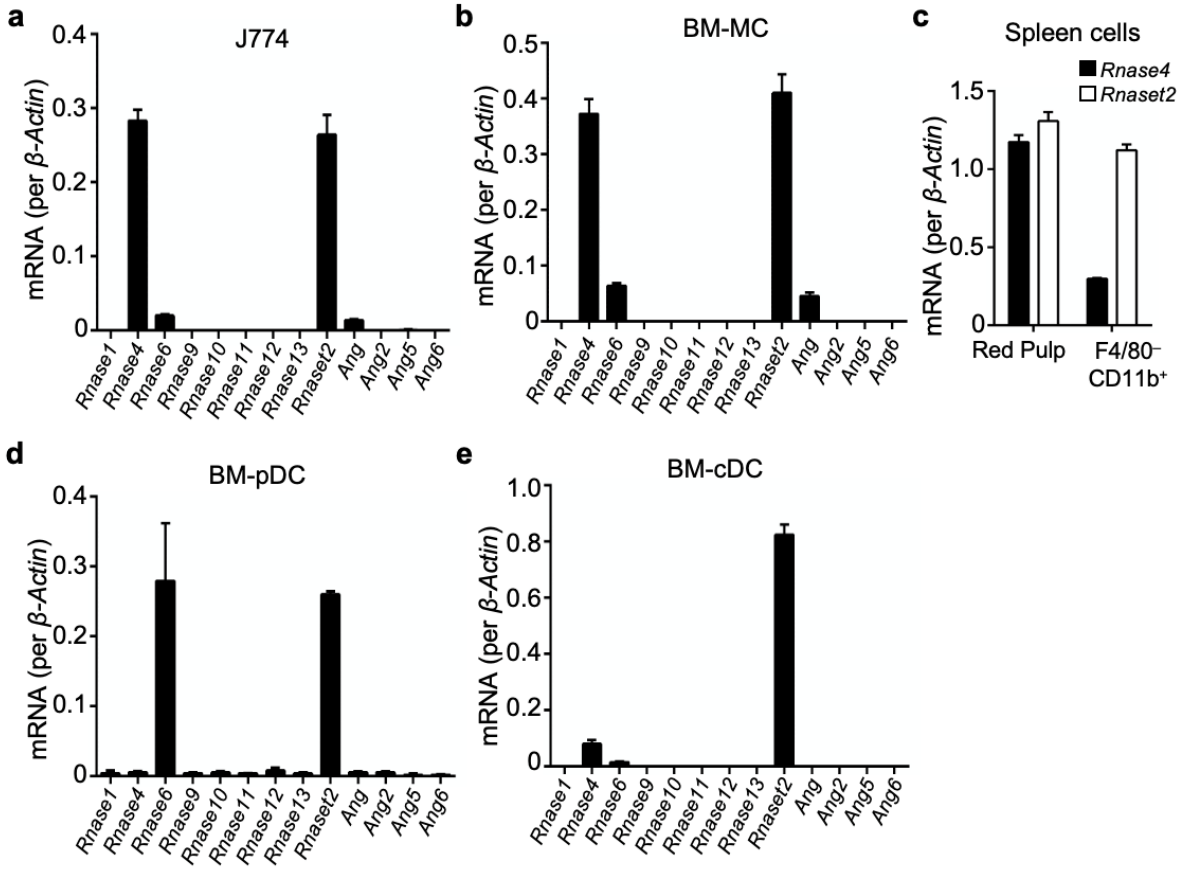

Figure 4. RNase mRNA expression in macrophages and bone marrow derived DCs. RNase mRNA expression in J774 (**a**), BM-MC (**b**), BM-pDC (**d**), and BM-cDC (**e**) are examined. (**c**) RNase4 and RNaseT2 mRNA expression in spleen F4/80$^+$ CD11b$^+$ red pulp macrophages and F4/80$^-$ CD11b$^+$ macrophages. The values are normalized by β-actin mRNA expression and represented by the averages with s.d. from triplicate wells.

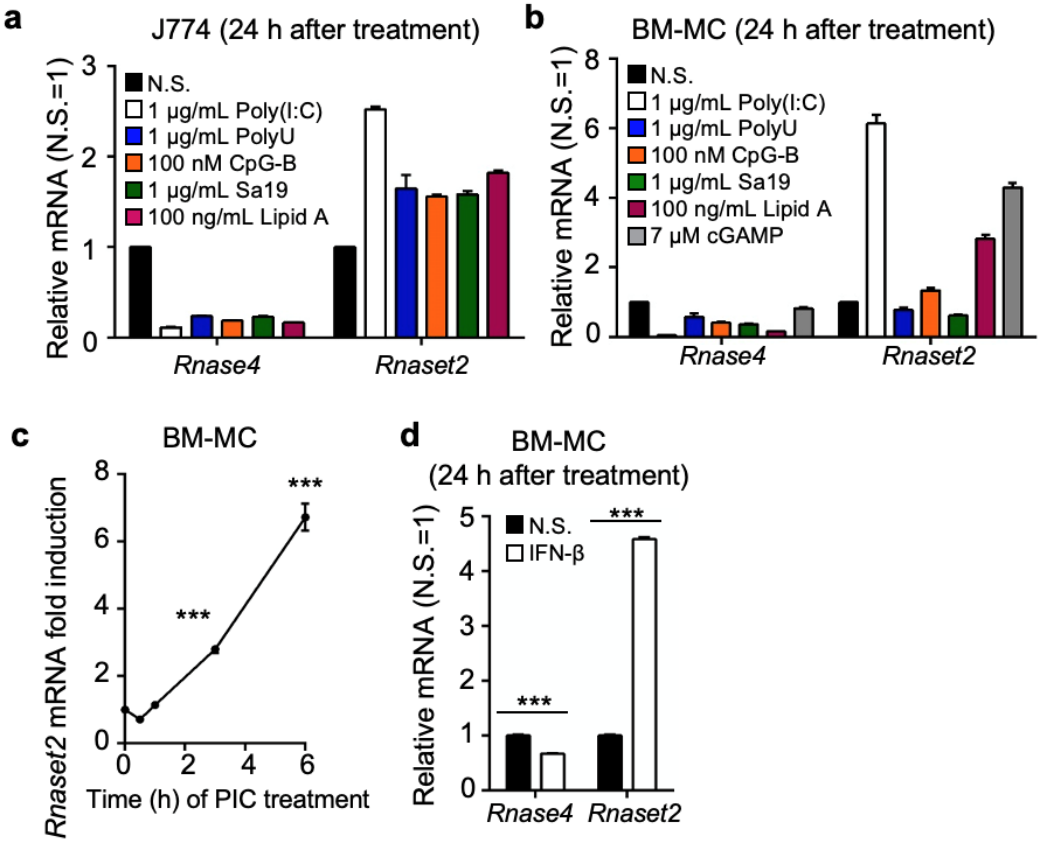

Figure 5. Induction of RNaseT2 mRNA and decrease in RNase4 mRNA by TLR ligands stimulation and IFN-β treatment. RNase4 and RNaseT2 mRNA expression in J774 (**a**) or BM-MC (**b**) after the cells were treated with indicated ligands for 24 hrs. The values are normalized by RNase mRNA expression in unstimulated cells and are represented by the averages with s.d. from triplicates. (**c**) RNA expression of RNaseT2 in BM-MCs after stimulation with poly(I:C) for indicated periods of times. The values are normalized by RNaseT2 mRNA expression in unstimulated cells and are represented by the averages with s.d. from triplicates. (**d**) mRNA expression of RNase4 and RNaseT2 in BM-MCs left untreated or treated for 24 with IFN-β at 200 U/mL. The values were normalized by mRNA expression in BM-MCs left untreated and represented by the averages with s.d. from triplicates. ***, $p<0.001$.

RNaseT2 differently impacted TLR3 and TLR7 responses

Based on the result above, *Rnase4*$^{-/-}$ J774 cell line and *Rnaset2*$^{-/-}$ J774 cell line was established utilizing CRISPR/Cas9 system by expressing sgRNA targeting genes encoding RNase4 or RNaseT2 and Cas9 protein into J774 cells. Genome editing was confirmed by analyzing PCR products from the genomic DNA. (Fig. 6a-b) The knockout of RNaseT2 was further confirmed at protein level by immunoblotting (Fig. 6c). Wild-type and *Rnase4*$^{-/-}$ cells were stimulated with RNA ligands including polyU and poly(I:C) at different concentrations and the production of CCL5, a typical chemokine expressed in immune responses, represented by the CCL5 concentration in the medium, was assessed by ELISA. The RNase4-deficient cells showed slightly lower CCL5 production in response to polyU compared to wild-type, while there were no changes in the responses to other RNA and non-RNA ligands (Fig. 7a). To investigate the impacts of RNaseT2-deficiency on immune response to RNA ligands, wild-type and *Rnaset2*$^{-/-}$ J774 cells were stimulated with the RNA ligands, and the production of CCL5 was assessed by ELISA. As a result, RNaseT2-deficiency increased the production of CCL5 in response to poly(I:C), and in contrast, decreased CCL5 production induced by polyU, without altering the responses to Lipid A (Fig. 7b). Consistent results were obtained in the mRNA level. The cells were stimulated by 1 μg/mL poly(I:C) or polyU, and then the mRNA of CCL5 was assessed by real-time PCR. Poly(I:C) stimulation induced higher CCL5 transcription in RNase-deficient cells (Fig. 7c). In contrast, CCL5 induction by polyU stimulation was impaired in the RNaseT2-deficient cells (Fig. 7d). In addition to CCL5 mRNA, IFN-β mRNA transcription was also increased at 3 hours or 6 hours after poly(I:C) stimulation in *Rnaset2*$^{-/-}$ J774 cells compared to wild-type cells (Fig. 7e).

To further study the role of RNaseT2 in primary macrophages, *Rnaset2*$^{-/-}$ mice were generated also with CRISPR/Cas9 system and confirmed at genome level with sequencing and protein level with immunoblotting (Fig. 8). Bone marrow cells from the mice were

allowed to differentiate into BM-MCs under the treatment of M-CSF. According to the expression of CD11b and CD11c, RNaseT2-defieciency did not change *in vitro* macrophage differentiation (Fig. 9a). Like J774, BM-MCs with RNaseT2-deficiency showed increased responses to poly(I:C) and decreased responses to polyU in the aspect of CCL5 or TNF-α production compared to wild-type BM-MCs, with no changes in response to R848, cGAMP or Lipid-A (Fig. 9b, 9c). Interestingly, poly(I:C)-dependent IFN-β mRNA induction was detected earlier and higher in *Rnaset2*$^{-/-}$ BM-MCs than in wild-type BM-MCs (Fig. 9d). To study the impact of RNaseT2-deficiency on immune response to viral infection, wild-type and *Rnaset2*$^{-/-}$ BM-MCs were infected with HSV-1, and then CCL5 and IFN-β expressions were assessed by real-time PCR. At mRNA level, the RNaseT2-deficienct cells showed a higher background expression, although the expressions after infection were also higher than wild-type cells (Fig. 9e).

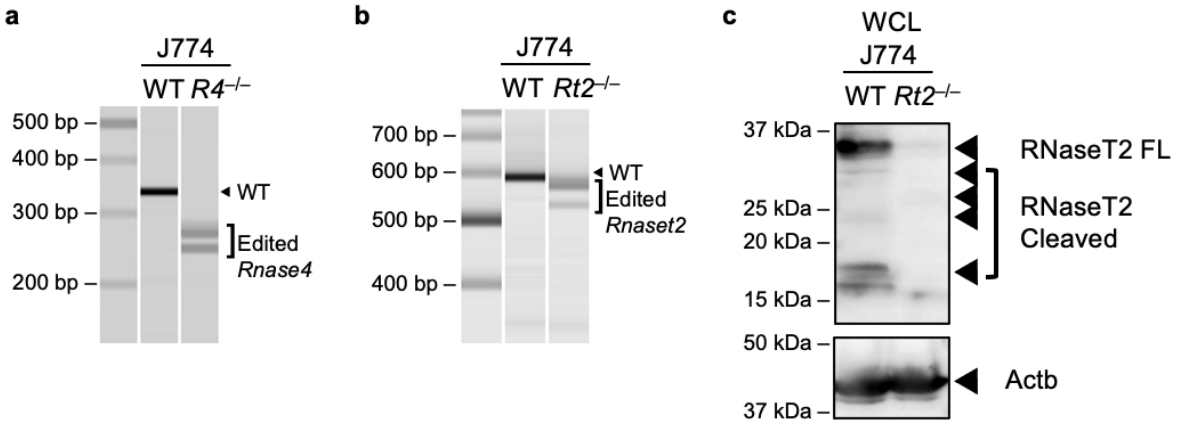

Figure 6. Confirmation of *Rnaset2*$^{-/-}$ J774 cells. (**a**) PCR products of the *Rnase4* gRNA check primer set from genomic DNA extracted from wild-type or *Rnase4*$^{-/-}$ J774 cells. (**b**) PCR products of the *Rnaset2* gRNA1 check primer set from genomic DNA extracted from wild-type or *Rnaset2*$^{-/-}$ J774 lines. (**b**) Immunoblotting of whole cell lysates from wild-type or *Rnaset2*$^{-/-}$ J774 lines with anti-RNaseT2 mAb. β-actin was also immunoprobed to show that amounts of samples are equal.

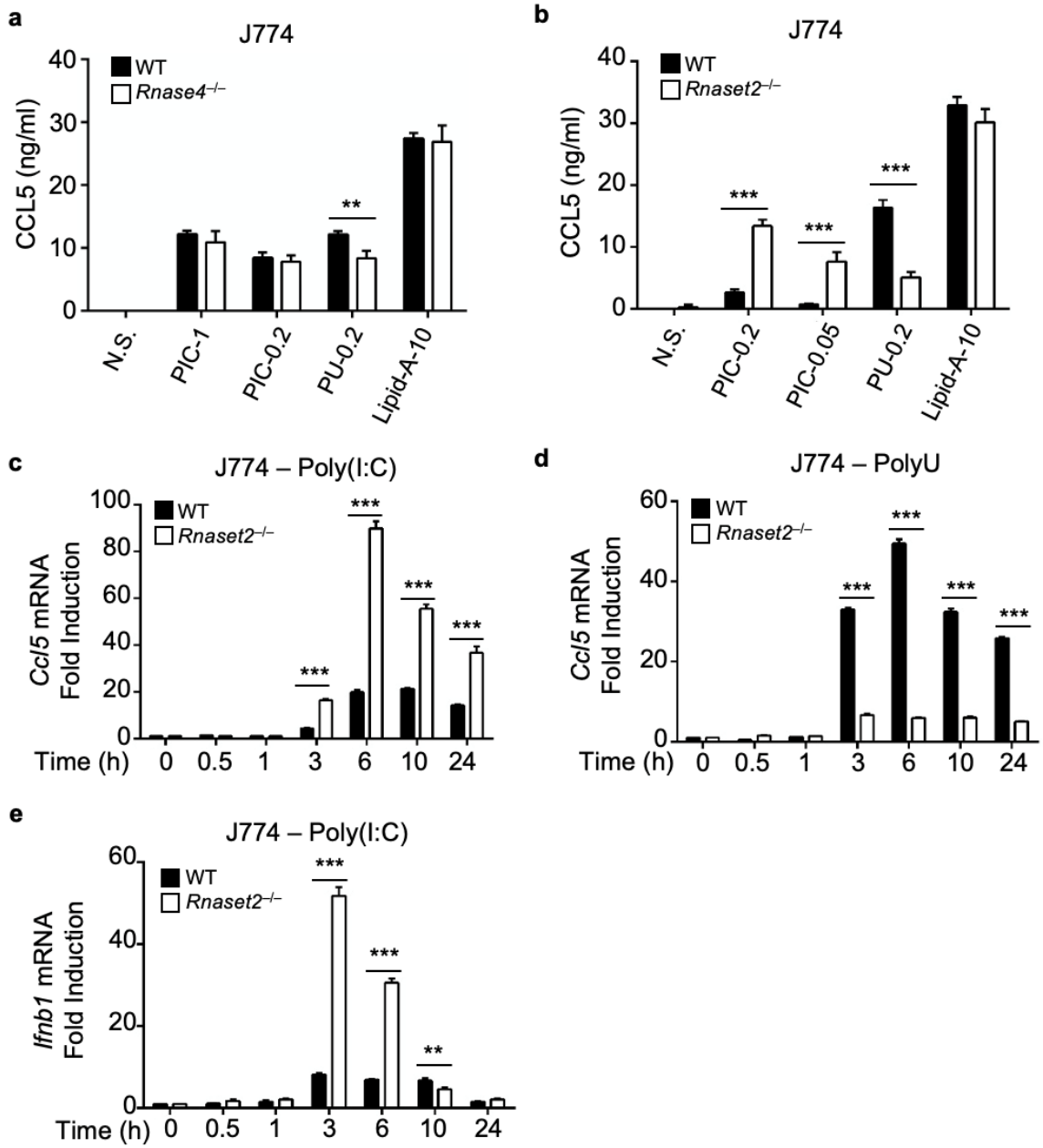

Figure 7. RNaseT2 downregulated TLR3 responses and upregulated TLR7 responses in J774 cells. Production of CCL5 by J774 cells after stimulation with indicated ligands for 24 h (**a**, **b**). The values were shown as the mean value with s.d. from triplicate wells. mRNA expression of CCL5 (**a**, **b**) or IFN-β (**d**) in J774 cells after stimulation with poly(I:C) (**a**, **d**) or polyU (**b**) at 1 μg/mL for indicated periods of times. The results of are shown as fold induction from the value of the cells left unstimulated. The values were shown as the mean value with s.d. from triplicate wells. **, $p< 0.01$. ***, $p<0.001$.

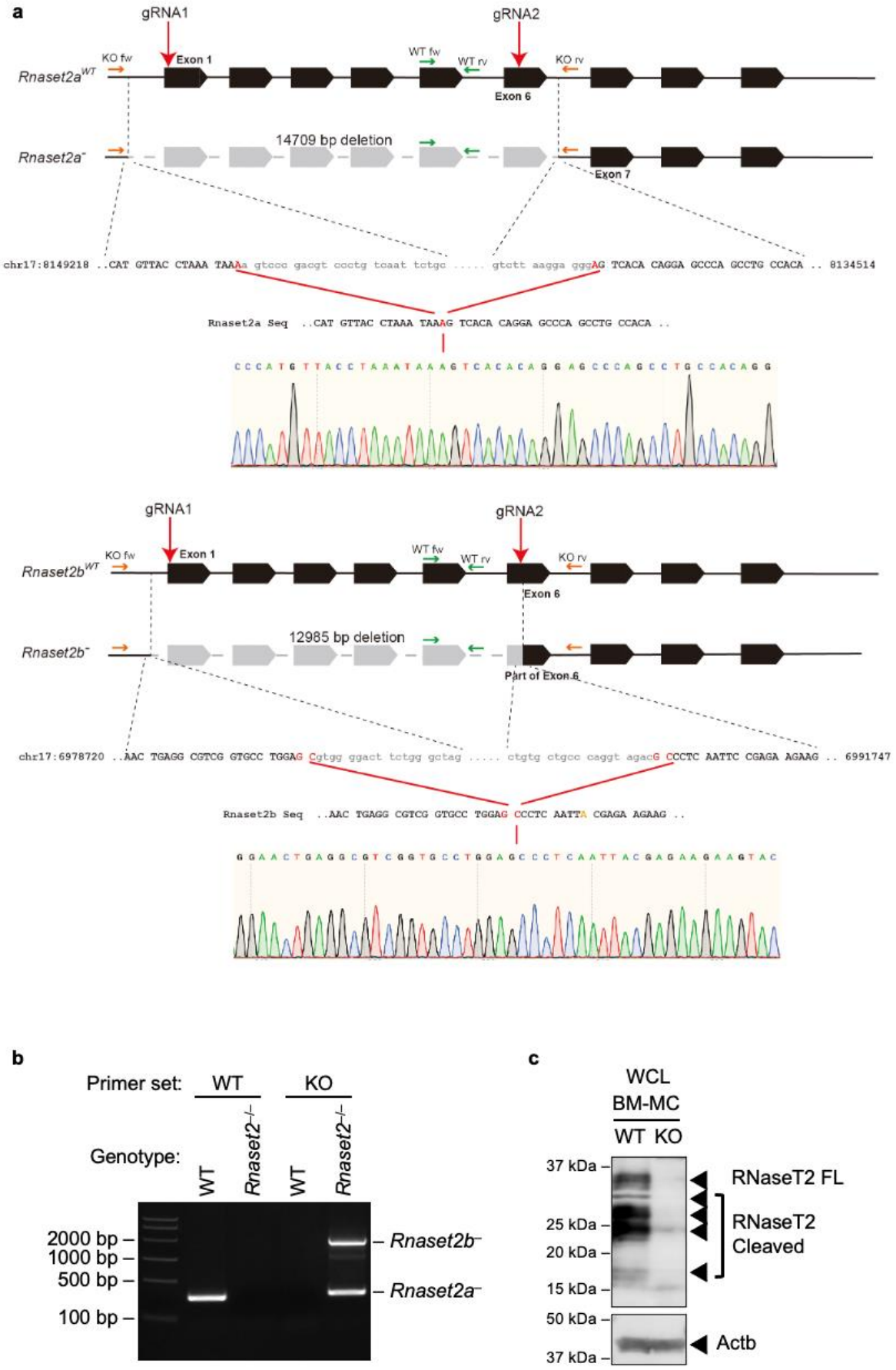
a
gRNA1
gRNA2
KO fw
Exon 1
WT fw
WT rv
KO rv
Exon 6
Rnaset2a^WT
14709 bp deletion
Rnaset2a⁻
Exon 7
chr17:8149218 ..CAT GTTAC CTAAA TAAAa gtccc gacgt ccctg tcaat tctgc ..... gtctt aagga gggAG TCACA CAGGA GCCCA GCCTG CCACA .. 8134514
Rnaset2a Seq ..CAT GTTAC CTAAA TAAAG TCACA CAGGA GCCCA GCCTG CCACA ..
gRNA1
gRNA2
KO fw
Exon 1
WT fw
WT rv
KO rv
Exon 6
Rnaset2b^WT
12985 bp deletion
Rnaset2b⁻
Part of Exon 6
chr17:6978720 ..AAC TGAGG CGTCG GTGCC TGGAG Cgtgg ggact tctgg gctag ..... ctgtg ctgcc caggt agacG CCCTC AATTC CGAGA AGAAG .. 6991747
Rnaset2b Seq ..AAC TGAGG CGTCG GTGCC TGGAG CCCTC AATTA CGAGA AGAAG ..
b
Primer set:
WT
KO
Genotype:
WT
Rnaset2⁻/⁻
WT
Rnaset2⁻/⁻
2000 bp –
1000 bp –
500 bp –
100 bp –
Rnaset2b⁻
Rnaset2a⁻
c
WCL
BM-MC
WT KO
37 kDa –
25 kDa –
20 kDa –
15 kDa –
RNaseT2 FL
RNaseT2
Cleaved
50 kDa –
37 kDa –
Actb

Figure 8. Generation and verification of *Rnaset2*$^{-/-}$ mice. (**a**) RNaseT2 was encoded by the two tandemly located genes, *Rnaset2a* and *Rnaset2b* in mice. Genomic configuration of the *Rnaset2a* and *Rnaset2b* genes is shown. The targeting sites of the gRNAs are indicated by red arrows. Deleted regions are shown. Orange and green arrows show the annealing sites of genotyping primers. (**b**) A typical genotyping result for wild-type and *Rnaset2*$^{-/-}$ mice. Because *Rnaset2a* and *Rnaset2b* genes were deleted differently, two PCR products were detected by genotyping of *Rnaset2*$^{-/-}$ mice. (c) Immunoblotting of whole cell lysates of wild-type or *Rnaset2*$^{-/-}$ BM-MCs with anti-RNaseT2 mAb. β-actin was also immunoprobed to show that amounts of samples are equal.

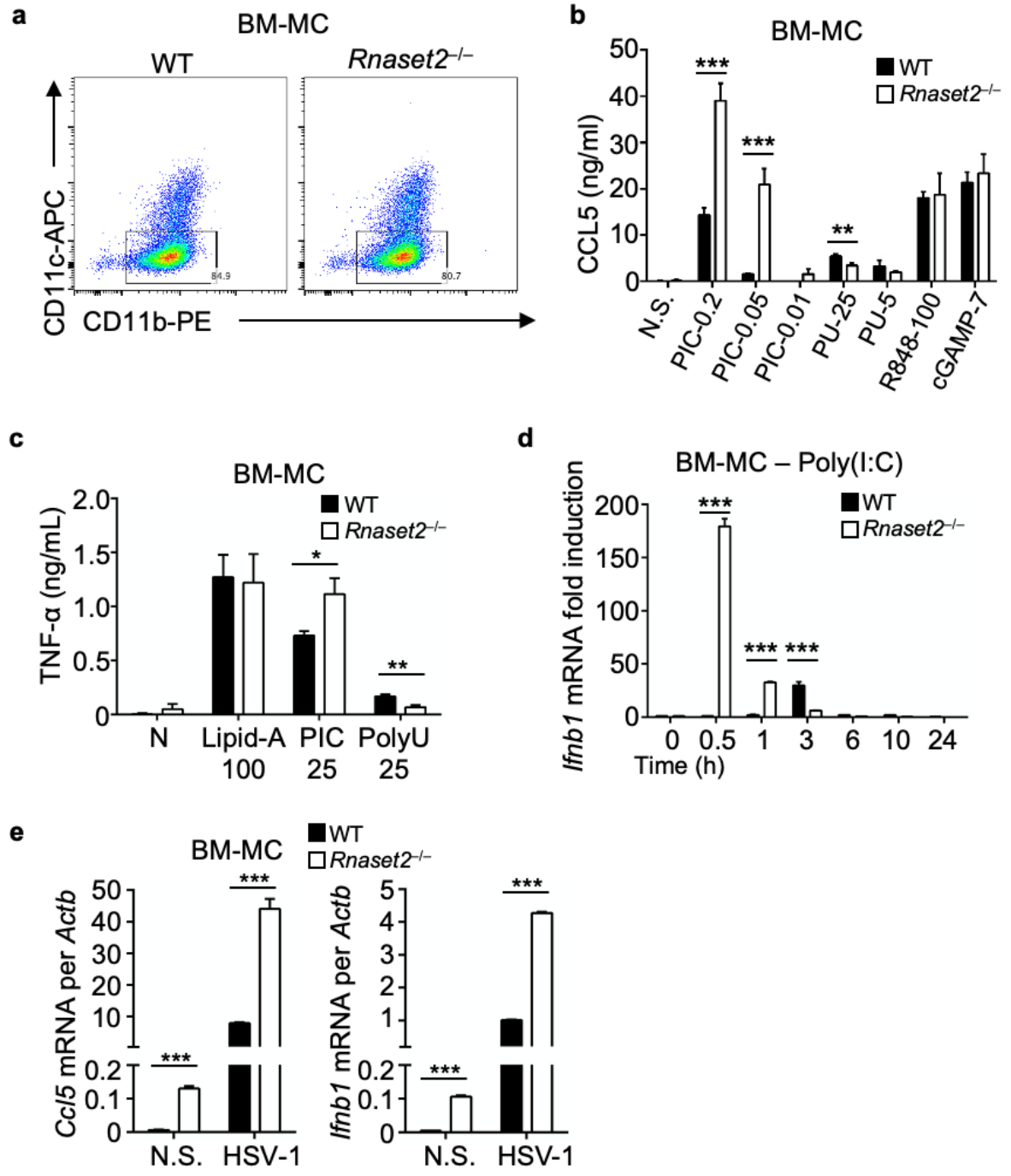

Figure 9. RNaseT2 downregulated TLR3 responses and upregulated TLR7 responses in BM-MCs. (**a**) Wild-type and *Rnaset2*$^{-/-}$ BM-MCs after the 1-week differentiation were stained with indicated antibodies to show expressions of the markers. Production of CCL5 (**b**) or TNF-α (**c**) by BM-MCs after stimulation with indicated ligands for 24 h. mRNA expression of CCL5 or IFN-β in BM-MCs after stimulation with poly(I:C) at 1 μg/mL for indicated periods of times (**d**) or infection with HSV-1 at MOI:5 for 6 h (**e**). The values were shown as the mean value with s.d. from triplicate wells. *, $p<0.05$. **, $p< 0.01$. ***, $p<0.001$.

As BM-cDCs and pDCs also express RNaseT2, the two types of cells were induced from bone marrow cells from wild-type and *Rnaset2*$^{-/-}$ mice and then stimulated with RNA ligands. Consistent with the macrophages, poly(I:C) induced increased CCL5 production in *Rnaset2*$^{-/-}$ BM-cDCs and the responses of BM-pDCs to polyU in CCL5 production were impaired by RNaseT2-deficiency (Fig. 10a, 10b). TLR7-dependent IFN-α productions in BM-pDCs induced by polyU and influenza virus A/Puerto Rico/8/34 (H1N1) (PR8)[74] were also abolished by RNaseT2-deficiency (Fig. 10c).

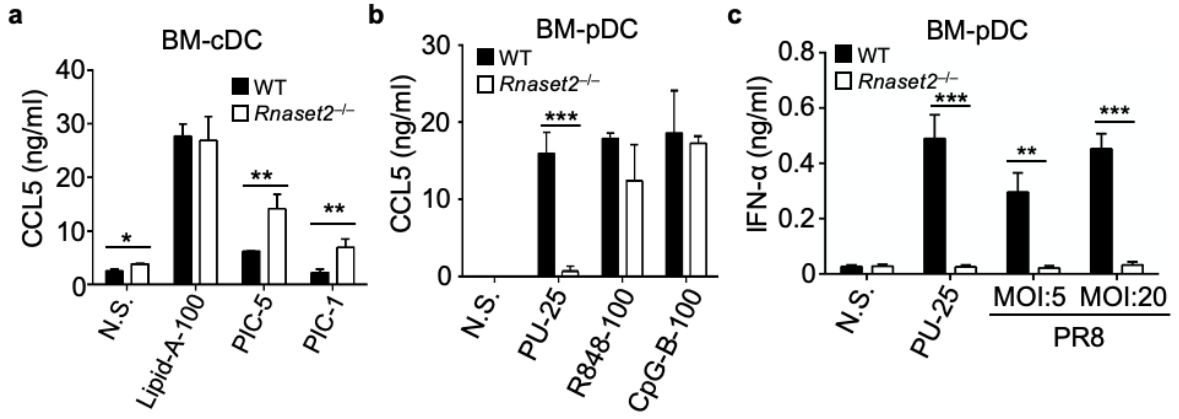

Figure 10. RNaseT2 downregulated TLR3 responses in BM-cDCs and is required for TLR7 responses in BM-pDCs. Production of CCL5 or IFN-α by BM-cDCs (**a**), or BM-pDCs (**b, c**) after stimulation with indicated ligands or infection with influenza virus A/Puerto Rico/8/34 (H1N1) (PR8) for 24 h. The values were shown as the mean value with s.d. from triplicate wells. *, $p<0.05$. **, $p<0.01$. ***, $p<0.001$.

To confirm that the enhanced poly(I:C) responses in *Rnaset2*$^{-/-}$ cells are TLR3-dependent, the J774 cells lacking both RNaseT2 and TLR3 were established (Fig. 11a). The increased CCL5 production in response to poly(I:C) stimulation in *Rnaset2*$^{-/-}$ J774 cells was completely abolished by the absence of TLR3, suggesting an enhanced TLR3 response in *Rnaset2*$^{-/-}$ cells (Fig. 11b).

These results strongly suggest that RNaseT2 negatively and positively regulates TLR3

and TLR7 responses, respectively, in macrophages and DCs.

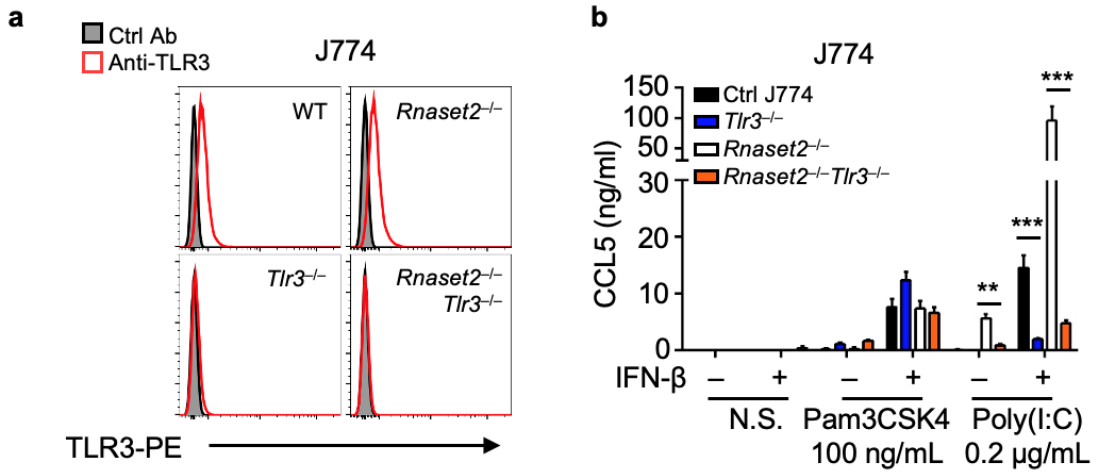

Figure 11. Hyperresponsiveness to poly(I:C) in *Rnaset2*$^{-/-}$ J774 was TLR3-dependent. (**a**) The lack of TLR3 in *Tlr3*$^{-/-}$ and *Rnaset2*$^{-/-}$ *Tlr3*$^{-/-}$ J774. Red histograms show TLR3 expression in indicated J774 lines. Gray histograms show staining with control Ab. (**b**) Indicated J774 lines were left untreated or treated with IFN-β at 200 U/mL for 6 h before stimulating with Pam3CSK4 at 100 ng/mL or poly(I:C) at 0.2 μg/mL. CCL5 production was evaluated with ELISA. The values were shown as the mean value with s.d. from triplicate wells. **, $p<0.01$. ***, $p<0.001$.

RNaseT2-deficiency did not alter TLR expression and RNA uptake in macrophages

The mechanism by which RNaseT2 impacted TLR responses was studied by examining three possibilities. RNaseT2 may regulate immune responses to RNA ligands by altering the expression of the receptors, influence the uptake or internalization of the ligands, or degrade RNA ligands.

The expression of TLR3 and TLR7 was examined in wild-type and *Rnaset2*$^{-/-}$ J774 cells and BM-MCs. Although the expression of TLR3 mRNA in BM-MCs and TLR7 mRNA in both types of cells were decreased in *Rnaset2*$^{-/-}$ cells (Fig. 12a, 12b), at protein level, FACS analyses failed to detect any alteration in the expression of TLR3 and TLR7 (Fig. 12c, 12d). After IFN-β treatment, TLR3 protein expression increased as reported previously,[75] whereas TLR7 protein expression was not changed (Fig. 12c, 12d). Despite

the upregulation of the expression of the receptor TLR3 itself and its negative regulator RNaseT2, TLR3-dependent CCL5 production in response to poly(I:C) was enhanced by Type I IFN (Fig. 11b). These results suggest that RNaseT2-deficiency did not alter the expression of TLR3 or TLR7 in macrophages.

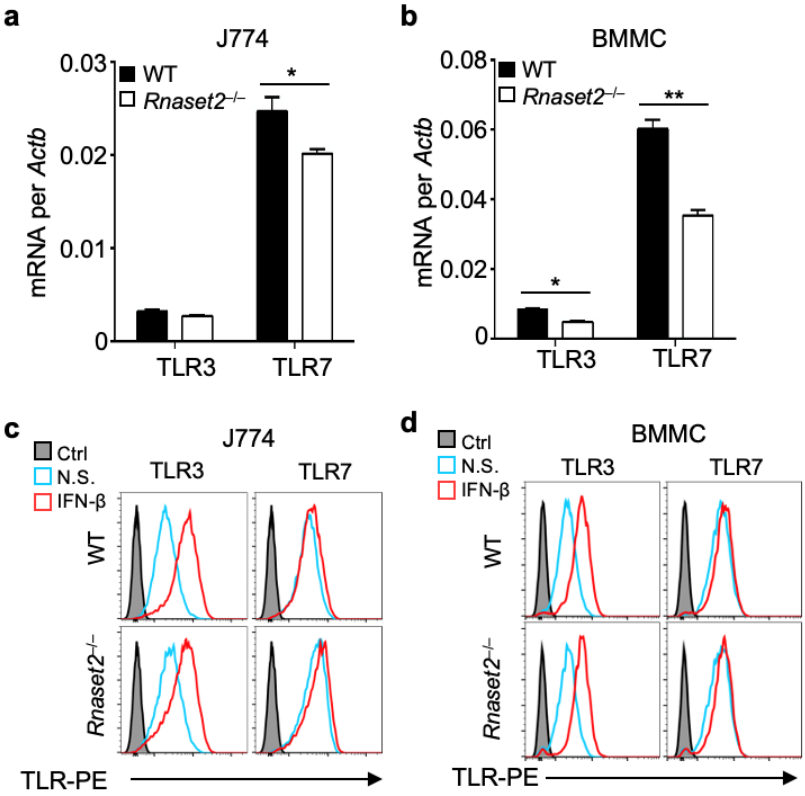

Figure 12. RNaseT2-deficiency did not increase TLR3 expression. Expression of mRNAs encoding TLR3 or TLR7 in wild-type or *Rnaset2*$^{-/-}$ J774 cells (**a**) or BM-MCs (**b**). The values are normalized by β-actin mRNA expression. The results are represented by the mean values with s.d. from triplicate wells. Expression of TLR3 and TLR7 in wild-type or *Rnaset2*$^{-/-}$ J774 cells (**c**) or BM-MCs (**d**) left untreated (blue histograms) or treated with 200 U/mL IFN-β for 24 h (red histograms) was evaluated by FACS analyses. Gray histograms show staining with a control Ab.

Next, the possibility that RNaseT2 is involved in RNA uptake was studied. Wild-type and *Rnaset2*$^{-/-}$ J774 cells were treated with rhodamine-labeled poly(I:C) for 30 min before FACS analyses. The fluorescence of poly(I:C) in *Rnaset2*$^{-/-}$ cells was not enhanced compared to wild-type cells indicating no enhanced poly(I:C) uptake in *Rnaset2*$^{-/-}$ cells

(Fig. 13).

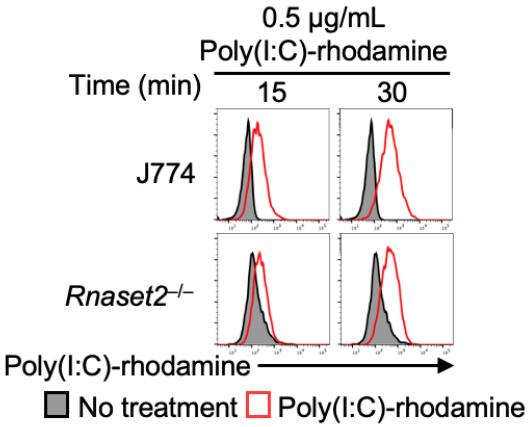

Figure 13. RNaseT2-deficiency did not increase RNA uptake. Indicated J774 lines were treated with poly(I:C) labelled with rhodamine for 15 or 30 m at 37°C. Bound poly(I:C)-rhodamine was detected by FACS analyses.

RNase activity of RNaseT2 is required for regulation of TLR responses

To address the last possibility that RNaseT2 degrade the RNA ligands, it is necessary to examine whether the RNase activity of RNaseT2 is required in its regulation on TLR responses.

First, wild-type RNaseT2 with a FLAG-His tag was purified by affinity chromatography (Fig. 14a) and applied to transfer RNA (tRNA), ssRNA with the stem-loop structure. The tRNA was found degraded after the treatment, indicating that the purified RNaseT2 with the tag did have RNase activity (Fig. 14b, 14c). Then, in total four mutants of RNaseT2 with FLAG-His tags were designed and purified (Fig. 14a). Three of these mutants - H69A, E118V and H122A - were designed by introducing mutations into the sites predicted to be required for the RNase activity.[61,76,77] Another mutant C188R was designed according to the human C184R mutant, which was reported to be linked with cystic leukoencephalopathy and of impaired RNase activity.[68] These purified mutated proteins were also applied to tRNA, and degradation was only found with H69A or E118V RNaseT2.

The H122A and C188R mutants failed to degrade the tRNA (Fig. 14b, 14c). These mutants or wild-type RNaseT2 were then transduced into the *Rnaset2*$^{-/-}$ J774 cells. The cells were stimulated with polyU. Despite comparable expression of these RNaseT2 proteins (Fig. 14d), impaired polyU-induced CCL5 production was only rescued by those with RNase activity - wild-type, H69A and E118V RNaseT2. H122A and C188R RNaseT2 proteins failed to rescue the TLR7 response to polyU (Fig. 14e). This suggests that the ssRNA digestion by RNaseT2 is required for TLR7 response.

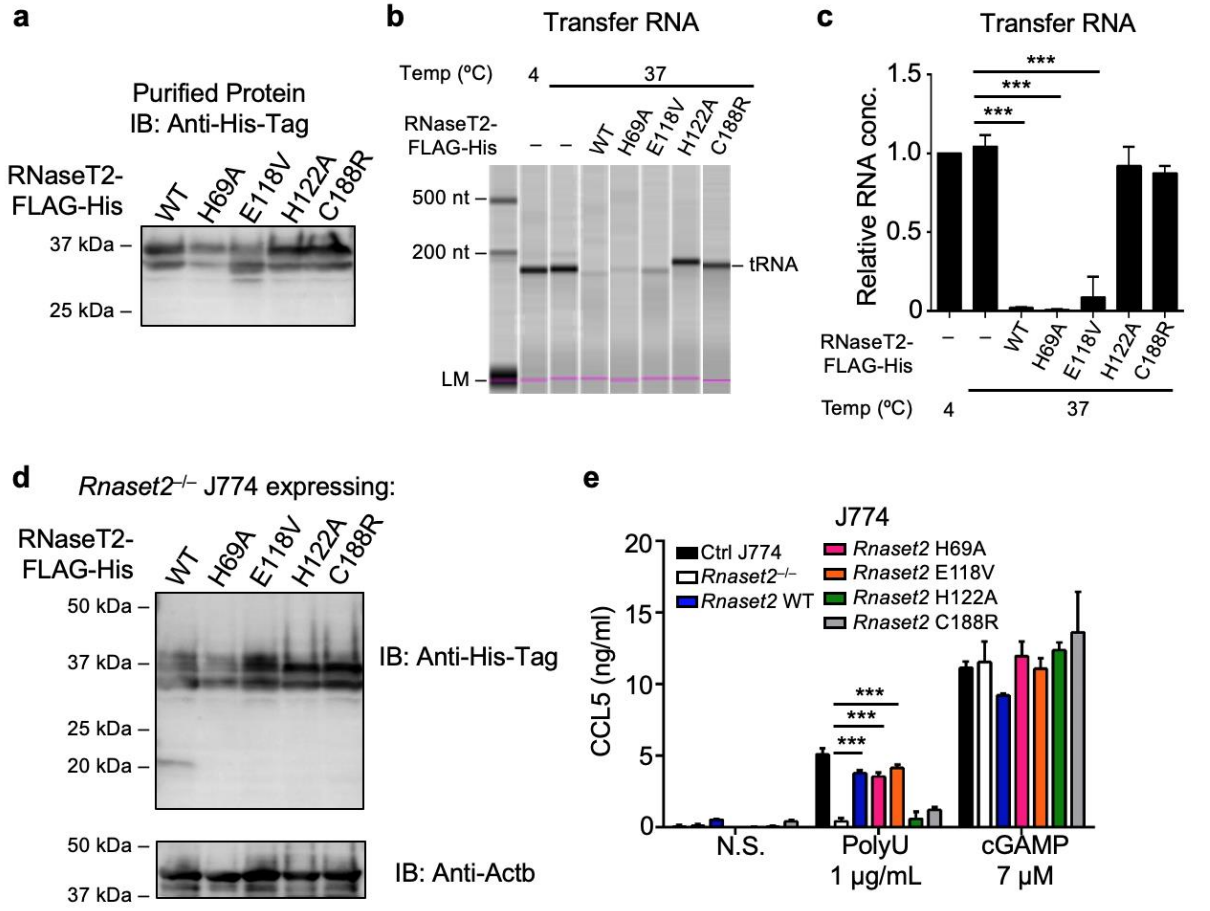

Figure 14. RNase activity of RNaseT2 was required for TLR7 responses. Immunoblotting with anti-His pAb of purified samples of indicated RNaseT2-Flag-His (**a**) or whole cell lysate of in *Rnaset2*$^{-/-}$ J774 lines expressing indicated RNaseT2-Flag-His. β-actin in the cells was also immunoprobed to show that amounts of samples are equal (**d**). tRNA as ssRNA were treated with 50 ng of purified RNaseT2 or its mutants for 1 h at 37 °C before capillary electrophoresis for tRNA (**b, c**). (**e**) CCL5 production after stimulation with polyU at 1 μg/mL or cGAMP at 7 μM for 24 h of *Rnaset2*$^{-/-}$ J774 cells complemented with wild-type RNaseT2

or RNaseT2 mutants. The results were represented by the mean values with s.d. from three independent experiments. ***, p<0.001

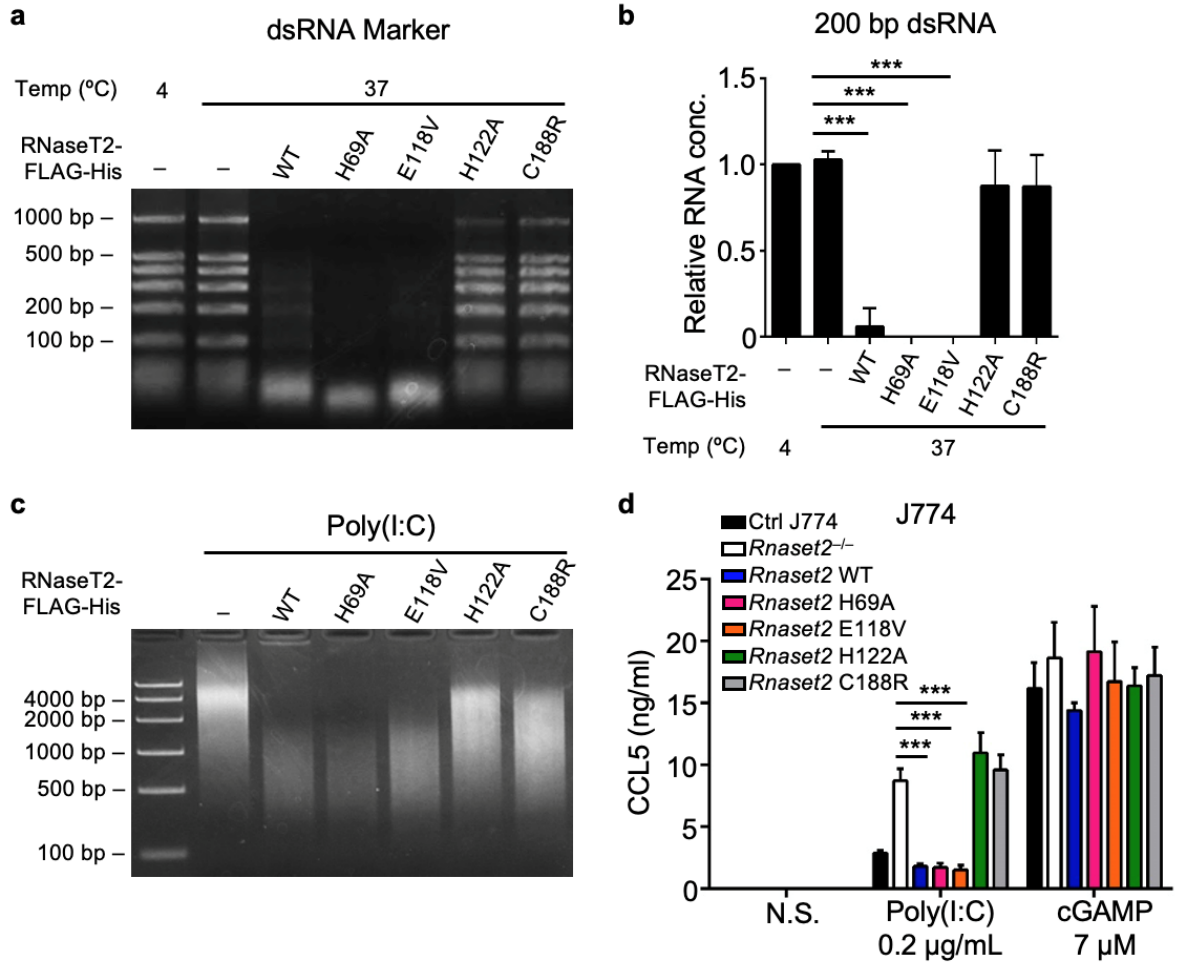

Figure 15. RNase activity of RNaseT2 was required for the negative regulation on TLR3 responses. dsRNA marker (**a**) or poly(I:C) (**c**) were treated with 50 ng of purified RNaseT2 or its mutants for 1 h at 37 °C before agarose electrophoresis. The amounts of 200 bp dsRNAs was evaluated with densitometry (**b**). The results were represented by the mean values with s.d. from three independent experiments. (**d**) CCL5 production after stimulation with poly(I:C) at 0.2 μg/mL or cGAMP at 7 μM for 24 h of *Rnaset2*$^{-/-}$ J774 cells complemented with wild-type RNaseT2 or RNaseT2 mutants. The results are represented by the mean values with s.d. from triplicate wells. ***, p<0.001.

As for dsRNA, it is widely believed that dsRNA is resistant to RNase digestion or degradation. However, in the experiment treating a commercial dsRNA marker with purified RNaseT2 proteins, degradation of the dsRNA was found with wild-type, H69A or E118V

RNaseT2 (Fig. 15a, 15b), indicating that RNaseT2 can digest dsRNA. Like the experiment with tRNA, H122A and C188R RNaseT2 proteins showed impaired RNase activity of the dsRNA. The dsRNA ligand poly(I:C) was also treated with the purified RNaseT2 proteins, and impaired digestion was only found with H122A and C188R RNaseT2 mutants (Fig. 15c). After stimulating the cells expressing wild-type or mutated RNaseT2 with poly(I:C), only H122A and C188R RNaseT2 expressing cells, as well as the *Rnaset2*$^{-/-}$ J774 cells exhibited upregulated CCL5 production (Fig. 15d). These results suggest that dsRNA digestion by RNaseT2 negatively regulates TLR3 responses.

RNaseT2 is localized in endosomes and lysosomes

To study the localization of endogenous RNaseT2 in BM-MCs, I separated cell organelles by density-gradient centrifugation and performed immunoblotting of RNaseT2 (Fig. 16). RNaseT2 was detected as multiple signals ranging from ~17 to ~35 kD. These signals were detected in the fractions positive for early endosome markers such as EEA1 and Rab5. The 35kD full-length signal was also detected in the fractions positive for late endosome / lysosome markers such as Lamp1 and Rab7a. Interestingly, overnight poly(I:C) stimulation increased the 35kD and 25kD signals in the fractions positive for late endosome / lysosomes markers, suggesting that RNaseT2 is transported to late endosomes / lysosomes upon stimulation with dsRNAs. TLR3 and TLR7 are also localized in these compartments.[14]

I next studied the subcellular distribution of RNaseT2 by confocal microscopy. Unfortunately, the anti-RNaseT2 mAb failed to detect endogenous RNaseT2 in confocal microscopy (Fig. 17a). I therefore examined RNaseT2-overexpressing J774 (Fig. 17b, 17c). RNaseT2 was detected as puncta in the cytoplasm and showed the highest colocalization with the late endosome/lysosome marker Lamp1, followed by the late endosome/lysosome marker Rab7a. No significant colocalization was found with the ER marker calnexin, the Golgi apparatus marker Golgin 97, or the early endosome markers, Rab5 or EEA1. Because

RNaseT2 was detected in the fractions positive for early endosome markers in density-gradient centrifugation (Fig. 16), RNaseT2 in early endosomes might not be detected in confocal microscopy. When J774 was stimulated with poly(I:C)-rhodamine, RNaseT2 was significantly colocalized with dsRNA poly(I:C) (Fig. 17b, 17c).

All these results above suggest that RNaseT2 is localized in the endosome or lysosome compartments to digest incorporated RNAs.

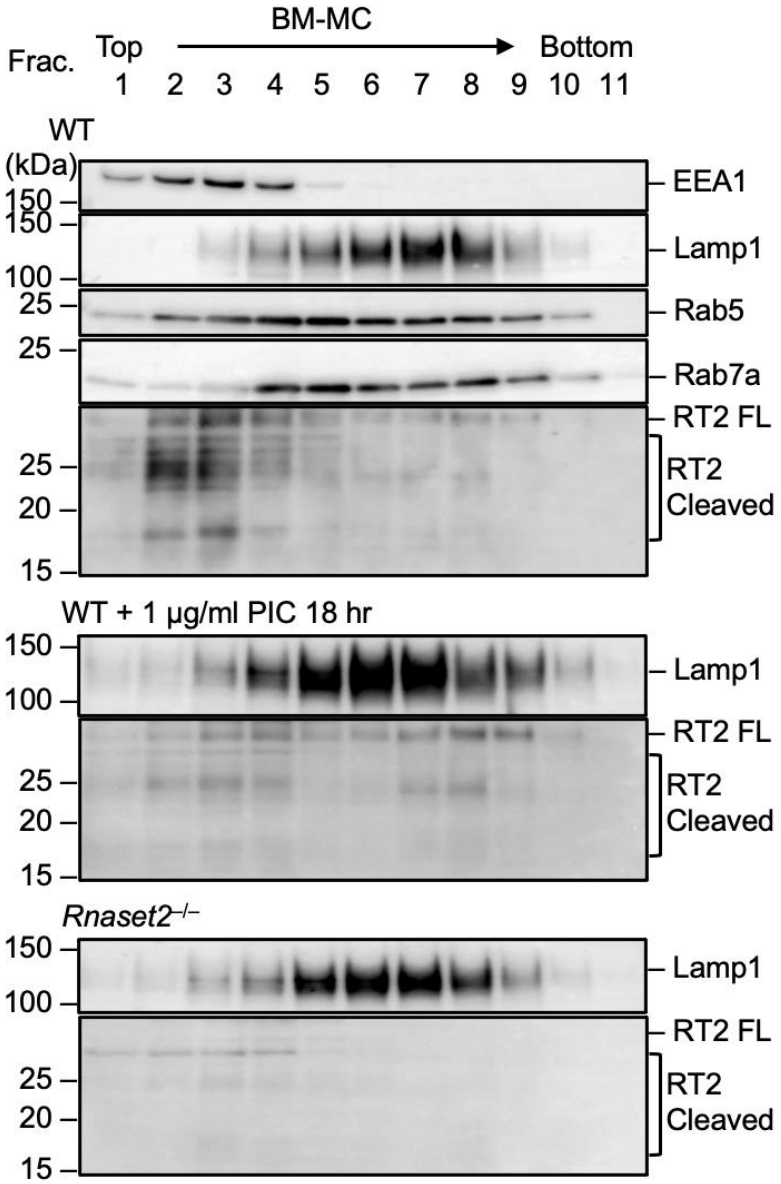

Figure 16. RNaseT2 was localized from endosomes to lysosomes. Immunoblotting of RNaseT2 and indicated organelle markers in the fractions prepared by density-gradient centrifugation of cell lysates from wild-type and *Rnaset2*$^{-/-}$ BM-MCs with or without

stimulation with poly(I:C) at 1 μg/mL for 18 hrs. Full-length and cleaved RNaseT2 are annotated as RT2 FL and RT2 Cleaved.

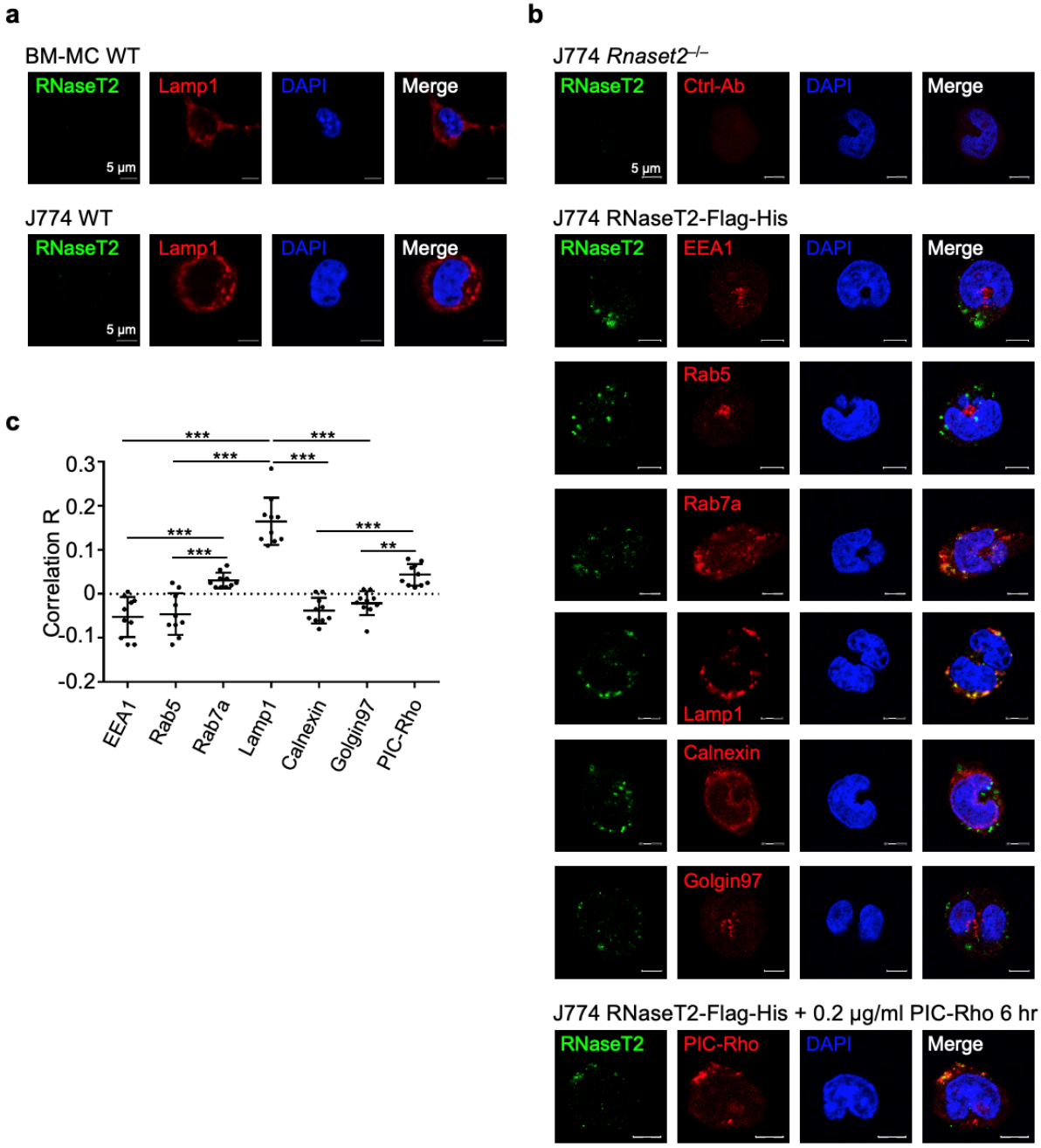

Figure 17. RNaseT2 was colocalized with endosome/lysosome markers and poly(I:C). (**a**) Wild-type BM-MCs and J774 cells were stained with anti-RNaseT2 mAb and Ab to Lamp1. Scale bar, 5 μm. (**b**) J774 cells over-expressing RNaseT2 were stained with anti-RNaseT2 mAb and Abs to indicated organelle-locating markers. The specificity of anti-RNaseT2 mAb was verified with *Rnaset2*$^{-/-}$ J774 cells. Scale bar, 5 μm. (**c**) Statistical analyses of colocalization of RNaseT2 with indicated markers are shown. **, p<0.01. ***, p<0.001.

Discussion

RNaseT2-regulated TLR responses

Here I showed that RNA degradation by RNaseT2 impacts endosomal RNA sensors (Fig. 18). Like human TLR8, TLR7 is probably to require a prior degradation of ssRNA to induce immune responses, as loss-of-function mutations of RNaseT2 impaired TLR7 responses to polyU and influenza virus, while RNaseT2-deficiency did not alter the responses to R848, a small molecular ligand to TLR7 and human TLR8. In human TLR8 responses, RNA digestion by RNaseT2 generates nucleoside,[56,72] and mouse TLR7 responses are also probably to depend on this.

In contrast to TLR7 responses, TLR3 responses are negatively regulated by RNaseT2. This negative regulation also requires the RNase activity of RNaseT2, as the mutants with impaired RNase activity on dsRNA marker or poly(I:C) were not able to downregulate the hyperresponsiveness to poly(I:C) in RNaseT2-deficient cells. In the experiment, RNaseT2 was able to digest dsRNA including the TLR3 ligand poly(I:C), although it is generally believed that dsRNA is resistant to RNase digestion.

RNaseT2 was previous reported to be localized in ER, lysosomes and mitochondrion intermembrane space or secreted to extracellular space.[63,65,71,78] In my study, endogenous RNaseT2 showed broad distribution ranging from early endosomes to late endosomes / lysosomes. Stimulation with poly(I:C) increased RNaseT2 in late endosomes / lysosomes. Such RNaseT2 trafficking is likely to enhance RNA degradation in the endosomal compartment and thereby negative regulation of TLR3 or enhancement of TLR7 responses. The colocalization of poly(I:C) and RNaseT2 within the cell was also confirmed. According to my result, it is likely that RNaseT2 degrades RNA ligand in late endosomes or lysosomes, but combining previous report on its extracellular localization, it is still possible

that the degradation happens before the ligands' entry to the cells. However, the RNaseT2 in fetal bovine serum did not compensate for the lack of RNaseT2 in the deficient cells. It is more likely that endosomes or lysosomes are the places for degradation or processing of the RNA ligands by RNaseT2.

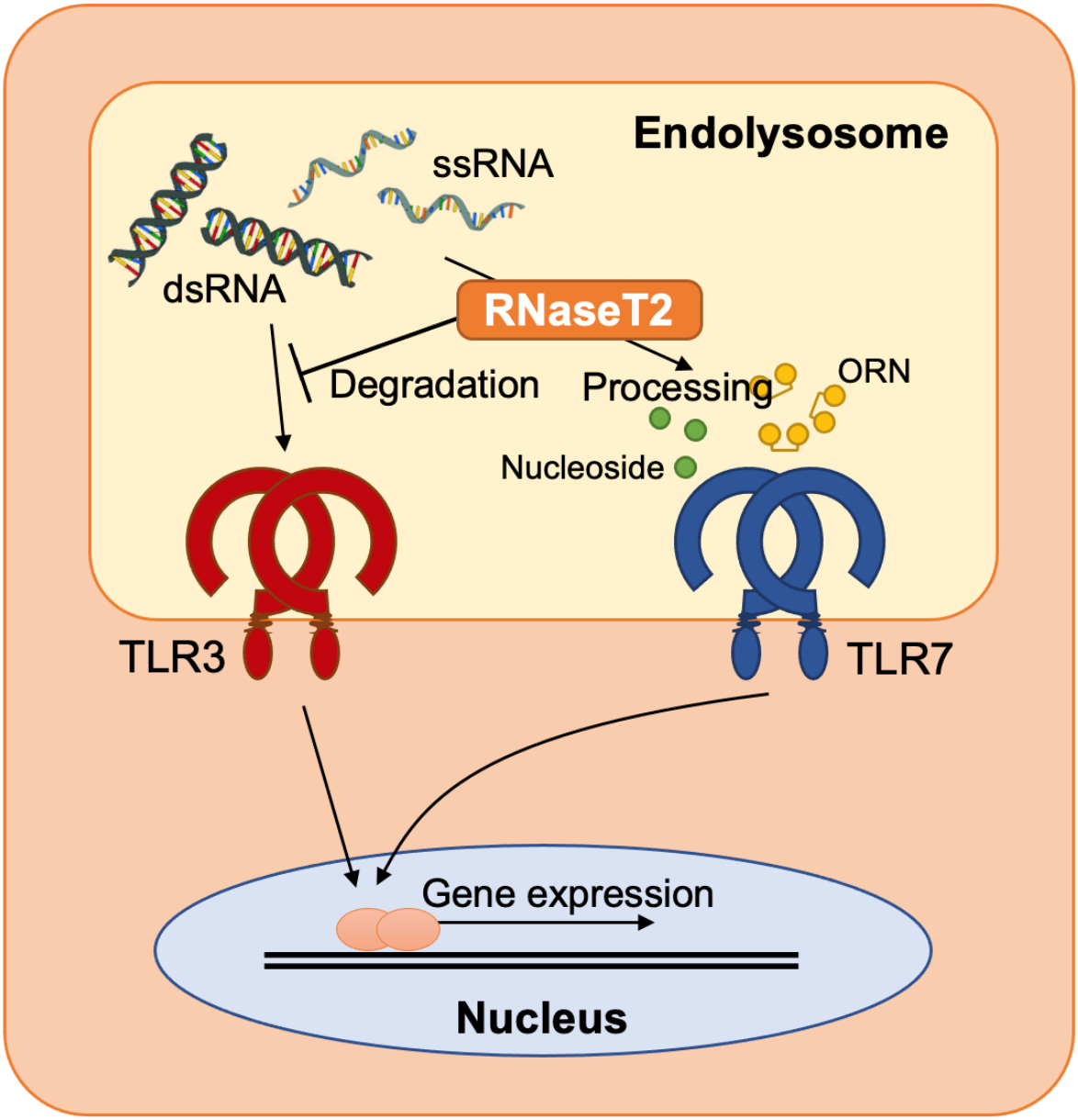

Figure 18. Roles of RNaseT2 in TLR3 and TLR7 responses. TLR7 responses are likely require prior digestion or processing of RNA ligands by RNaseT2. TLR3 responses to dsRNA are negatively regulated by RNaseT2 through degrading the ligands.

In my study, I found that ligand stimulation and Type I IFN induced RNaseT2 mRNA transcription, indicating that RNaseT2 might have roles in defense responses against viruses, when Type I IFNs are produced. In this context, TLR7 responses are likely to be upregulates by the increased RNaseT2 expression, resulting in more efficient production of ligands, i.e., guanosine and UUU ORN, for the receptor. Simultaneously, TLR3 responses were also enhanced by Type I IFN treatment despite the increased expression of RNaseT2, the negative regulator of TLR3 responses. This might be explained by the increased TLR3 expression induced by Type I IFN. These results suggest that Type I IFNs increase macrophage responses to RNA by increasing the expression of TLR3, an RNA sensor, and RNaseT2, an enzyme generating ligands for other RNA sensors like TLR7 and human TLR8.

RNA digestion by RNaseT2 had opposite impacts on TLR3 and TLR7, and tissue-resident macrophages such as red pulp macrophages in spleen, in which I have shown the expression of RNaseT2, microglia in brain, alveolar macrophages in lung and cardiac macrophages express both TLR3 and TLR7.[79] In these macrophages RNaseT2 is likely to skew the balance of endosomal responses to RNA from TLR3 to TLR7.

As for the enzymatic activity of RNaseT2, the purified RNaseT2 was proved to be enzymatical active and able to digest both single-stranded and double-stranded RNAs. The histidine at Position 122 was identified as vital in its capability of RNA degradation. In human, histidine at Position 118, corresponding the histidine at Position 122 of mouse RNaseT2, abolishes the effect on degradation of mitochondrion associated cytosolic RNAs. As well, the mutant C188R of mouse RNaseT2, mimicking human C184R mutant linked with leukoencephalopathy, has an impaired enzymatic activity. This is consistent with the previous report testing the enzymatic activity of human wild-type and C184R RNaseT2 proteins.[68,69] These two sites, the histidine and the cystine, are indispensable for the enzymatic activity of RNaseT2.

Roles of nucleases in immune responses

The role of RNaseT2 in the macrophage TLR3 and TLR7 responses was studied here, which suggested different roles of RNases in the immune responses of RNA sensors. As is reported before, an RNase in the human RNase A family called RNase2 is also required for human TLR8 response to ssRNA in addition to RNaseT2.[56,72]

In my study, the expression of RNase4 in macrophages was also confirmed, and with ligand stimulation or Type I IFN treatment, RNase4 mRNA level was downregulated. It is possible that RNase4 also play roles in immune responses, but RNase4 failed to compensate for the lack of RNaseT2 in TLR3 and TLR7 responses, demonstrating a nonredundant role of RNaseT2 in these responses. It may be due to the extracellular localization of RNase4. The RNase4-deficient cells showed slightly lower response to TLR7 ligand polyU. A reasonable reason for this phenotype is that RNase4 is a secreted protein and the fetal bovine serum RNase4 compensated for the lack of RNase4 expression within the *Rnase4*$^{-/-}$ cells. Meanwhile, RNase6 is another RNase of lysosomal and extracellular localization, and according to my result, RNase6 is expressed, though relatively low, in macrophages. It has been reported that RNase6 has antimicrobial function in human or murine urinary tract and skin.[57] It is also possible that RNase6 is involved in some immune responses to bacterial or viral RNA.

As for other dsRNA sensors like RIG-I or MDA5 localized in cytoplasm, there are also possibilities that RNaseT2 or other RNases are involved in their responses to RNA. Since dsRNA in endosomal compartments can be transported to cytoplasm through the transporter Sidt2,[80] dsRNA digestion by RNaseT2 might also negatively regulates the activation of these cytoplasmic dsRNA sensors in addition to TLR3. Endogenous retrovirus-derived dsRNA is released from nucleus and thus activate MDA5 and TLR3.[81] Innate immune responses to cytoplasmic dsRNA are inhibited by ADAR1 through A to I

RNA editing, which generates mismatch loops in dsRNA.[82] Since cytoplasmic dsRNA can also enter the endosomal compartments via autophagy or the transporter Sidt2,[80] ADAR1 generated mismatch loops may make dsRNA more susceptible to digestion by RNases. In this case, RNaseT2-degestion might work together with ADAR1 or Sidt2 to regulate TLR3 responses to cytoplasmic dsRNA.

My laboratory previously showed that DNase II is required for TLR9 responses to CpG-A.[51] Nucleic acid recognition by endosomal TLR3, TLR7, TLR8, and TLR9 all depends on nucleic acid degradation in endosomal compartments, demonstrating a reason why these TLRs need to reside in endosomal compartments, where nucleic acids are degraded. RNA degradation is tightly linked with RNA-sensing by endosomal TLRs.

RNaseT2 and leukoencephalopathy

The loss-of-function mutant of RNaseT2, C184R is linked with the human disease, cystic leukoencephalopathy without megalencephaly.[68,69] In my study, I also found the C188R mutant in mouse, corresponding the human mutant, of impaired enzymatic activity. As a result, it is not sufficient for RNA digestion or processing in endolysosomes, leading to upregulated TLR3 responses and impaired TLR7 responses. As microglia express both TLR3 and TLR7,[79] microglia harboring the human C184R / mouse C188R RNaseT2 mutation is likely to show more robust TLR3 responses and weaker TLR7 responses than wild-type microglia, which may serve as possible explanation to the link of RNaseT2-deficiency to leukoencephalopathey. According to previous reports, there are similarities between cystic leukoencephalopathy without megalecyphaly and the Type I interferonopathy Aicardi-Goutières syndrome.[63,69] Microglia-specific expression of RNaseT2 rescued the disease phenotypes in RNaseT2-deficient zebrafish.[71] Since RNaseT2-deficiency led to higher TLR3-dependent transcription of IFN-β in my study, these previous reports suggest that TLR3 hyperresponsiveness in microglia might have

pathogenic roles in the disease. Moreover, as cells like neurons also express TLR3, RNaseT2-deficiency may lead to TLR3 hyperresponsiveness in neurons, as well, which probably contributes to the disease. This should be studied further to reveal the link between RNaseT2-deficiency and leukoencephalopathy.

Acknowledgement

First, I would like to express my sincere thanks to my supervisor, Prof. Kensuke Miyake, Division of Innate Immunity, the Institute of Medical Science, the University of Tokyo, who has given me much indispensable tutelage and encouragement during my study in the laboratory for the past five years.

On detailed problems in the study and experiments, Dr. Ryota Sato advised me a lot. Hereby, I would like to give my special thanks to him. Also, I would like to give my thanks to Dr. Takuma Shibata who constructed the *Rnaset2*$^{-/-}$ mouse, and Ryosuke Hiranuma, Tatjana Reuter, and Dr. Yun Zhang for their help in the experiment. I also appreciate Dr. Ryutaro Fukui and Dr. Shin-Ichiroh Saitoh for their help me in the optimization of antibody concentrations and some techniques during my experiment using antibodies and confocal microscope. And thanks to other members of the Division of Innate Immunity, for their helps and discussions on my study. It is absolutely meaningful five years for me to have studied here in this laboratory.

I would also express my thanks to Associate Prof. Takeshi Ichinohe of the Department of Infectious Disease Control, International Research Center for Infectious Diseases, IMSUT, as well as Dr. Akihisa Kato and Prof. Yasushi Kawaguchi of the Division of Molecular Virology, IMSUT. They have kindly helped me with influenza virus and herpes simplex virus infection experiments. I want to give my thanks to Prof. Eicke Latz from Institute of Innate Immunity, Biomedical Center, University of Bonn for his advice on this study.

Besides, I want to say thanks to two of my best friends for listening to my complaint every time when I came into problems in study or in life and giving me much advice. One of them is going to the United States for his PhD course this year, two years after he finished

his master course there. I hope that he can get his PhD degree smoothly, and that he is able to visit me here in Japan on his trip to the States. The other is now still in Shanghai, who have resigned from his master course at Fudan right after his first visit to Japan. I still feel sorry that I could not help him when he burst into tears at Odaiba that time. Although it is still not widely accepted, I hope that he can get along well with his boyfriend.

Last but not the least, I have a lot of thanks to my parents and my whole family. Without their full support, it is impossible for me to finish my current study. I fully understand that they are almost always concerned about my safety and health. As the COVID-19 pandemic has stopped many people from travel beyond borders, it gets more difficult for me to reunite with them. The last time I went back to China is January 2020, when the pandemic just started. Back then, I, like most people, did not realize that the SARS-like disease could make so great changes to the whole world. Shutdown of borders, strict quarantines, lockdown of cities or prefectures and vaccination, all these the actions taken by governments, which are supposed to contribute to containing of the virus, have built high walls among countries as side effects. Even worse, the political viruses, the rumors, and false accusations, spread by certain politicos, have built walls among people from different countries. I hope that with the penetration of vaccine, the travel beyond borders will resume soon. As an international student, I believe that only constructive communications can break down the walls built by the viruses. I strongly recommend that after the pandemic people should try to go somewhere abroad, not only those places for vacation, but also the places they commented without experiencing the place themselves, to re-educate themselves with the rapidly changing world. Finally, back to the hope for myself, I am really looking forward to the reunites with my parents, my grandparents, and my friends, hopefully soon.

References

1 Murphy, K. & Weaver, C. *Janeway's immunobiology*. (Garland Science, 2016).

2 Miyake, K. & Kaisho, T. Homeostatic inflammation in innate immunity. *Current Opinion in Immunology* **30**, 85, doi:10.1016/j.coi.2014.08.003 (2014).

3 Heine, H. & Lien, E. Toll-like receptors and their function in innate and adaptive immunity. *Int Arch Allergy Immunol* **130**, 180-192, doi:10.1159/000069517 (2003).

4 Ezekowitz, R. A. B. & Hoffmann, J. A. *Innate immunity*. (Springer Science & Business Media, 2002).

5 Akira, S., Uematsu, S. & Takeuchi, O. Pathogen recognition and innate immunity. *Cell* **124**, 783-801, doi:10.1016/j.cell.2006.02.015 (2006).

6 Christensen, S. R. *et al.* Toll-like receptor 7 and TLR9 dictate autoantibody specificity and have opposing inflammatory and regulatory roles in a murine model of lupus. *Immunity* **25**, 417-428, doi:10.1016/j.immuni.2006.07.013 (2006).

7 Deane, J. A. *et al.* Control of toll-like receptor 7 expression is essential to restrict autoimmunity and dendritic cell proliferation. *Immunity* **27**, 801-810, doi:10.1016/j.immuni.2007.09.009 (2007).

8 Kawai, T. & Akira, S. The role of pattern-recognition receptors in innate immunity: update on Toll-like receptors. *Nat Immunol* **11**, 373-384, doi:10.1038/ni.1863 (2010).

9 Kawai, T. & Akira, S. Signaling to NF-kappaB by Toll-like receptors. *Trends Mol Med* **13**, 460-469, doi:10.1016/j.molmed.2007.09.002 (2007).

10 Beutler, B. *et al.* Genetic analysis of host resistance: Toll-like receptor signaling and immunity at large. *Annu Rev Immunol* **24**, 353-389, doi:10.1146/annurev.immunol.24.021605.090552 (2006).

11 Bsibsi, M., Ravid, R., Gveric, D. & van Noort, J. M. Broad expression of Toll-like

receptors in the human central nervous system. *J Neuropathol Exp Neurol* **61**, 1013-1021 (2002).

12 Lemaitre, B., Nicolas, E., Michaut, L., Reichhart, J. M. & Hoffmann, J. A. Pillars article: the dorsoventral regulatory gene cassette spatzle/Toll/cactus controls the potent antifungal response in Drosophila adults. Cell. 1996. 86: 973-983. *J Immunol* **188**, 5210-5220 (2012).

13 Medzhitov, R., Preston-Hurlburt, P. & Janeway, C. A., Jr. A human homologue of the Drosophila Toll protein signals activation of adaptive immunity. *Nature* **388**, 394-397, doi:10.1038/41131 (1997).

14 Miyake, K. *et al.* Mechanisms controlling nucleic acid-sensing Toll-like receptors. *International Immunology* **30**, 43, doi:10.1093/intimm/dxy016 (2018).

15 Blasius, A. L. & Beutler, B. Intracellular toll-like receptors. *Immunity* **32**, 305-315, doi:10.1016/j.immuni.2010.03.012 (2010).

16 Botos, I., Segal, D. M. & Davies, D. R. The structural biology of Toll-like receptors. *Structure* **19**, 447-459, doi:10.1016/j.str.2011.02.004 (2011).

17 Nagai, Y. *et al.* Essential role of MD-2 in LPS responsiveness and TLR4 distribution. *Nat Immunol* **3**, 667-672, doi:10.1038/ni809 (2002).

18 Oldenburg, M. *et al.* TLR13 recognizes bacterial 23S rRNA devoid of erythromycin resistance-forming modification. *Science (New York, N.Y.)* **337**, 1111, doi:10.1126/science.1220363 (2012).

19 Fitzgerald, K. A. *et al.* LPS-TLR4 signaling to IRF-3/7 and NF-kappaB involves the toll adapters TRAM and TRIF. *J Exp Med* **198**, 1043-1055, doi:10.1084/jem.20031023 (2003).

20 Yamamoto, M. *et al.* Cutting edge: a novel Toll/IL-1 receptor domain-containing adapter that preferentially activates the IFN-beta promoter in the Toll-like receptor signaling. *J Immunol* **169**, 6668-6672 (2002).

21 Yamamoto, M. *et al.* TRAM is specifically involved in the Toll-like receptor 4-mediated MyD88-independent signaling pathway. *Nat Immunol* **4**, 1144-1150, doi:10.1038/ni986 (2003).

22 Fukui, R. *et al.* Unc93B1 biases Toll-like receptor responses to nucleic acid in dendritic cells toward DNA- but against RNA-sensing. *J Exp Med* **206**, 1339-1350, doi:10.1084/jem.20082316 (2009).

23 Kim, Y. M., Brinkmann, M. M., Paquet, M. E. & Ploegh, H. L. UNC93B1 delivers nucleotide-sensing toll-like receptors to endolysosomes. *Nature* **452**, 234-238, doi:10.1038/nature06726 (2008).

24 Tabeta, K. *et al.* The Unc93b1 mutation 3d disrupts exogenous antigen presentation and signaling via Toll-like receptors 3, 7 and 9. *Nat Immunol* **7**, 156-164, doi:10.1038/ni1297 (2006).

25 Jong, S. D. d. *et al.* The Immunostimulatory Activity of Unmethylated and Methylated CpG Oligodeoxynucleotide Is Dependent on Their Ability To Colocalize with TLR9 in Late Endosomes. *The Journal of Immunology* **184**, 6092, doi:10.4049/jimmunol.0802442 (2010).

26 Ishikawa, H. & Barber, G. N. STING is an endoplasmic reticulum adaptor that facilitates innate immune signalling. *Nature* **455**, 674-678, doi:10.1038/nature07317 (2008).

27 Ishikawa, H., Ma, Z. & Barber, G. N. STING regulates intracellular DNA-mediated, type I interferon-dependent innate immunity. *Nature* **461**, 788-792, doi:10.1038/nature08476 (2009).

28 Zhang, Z. *et al.* Structural Analysis Reveals that Toll-like Receptor 7 Is a Dual Receptor for Guanosine and Single-Stranded RNA. *Immunity* **45**, 737-748, doi:10.1016/j.immuni.2016.09.011 (2016).

29 Tanji, H., Ohto, U., Shibata, T., Miyake, K. & Shimizu, T. Structural reorganization of

the Toll-like receptor 8 dimer induced by agonistic ligands. *Science* **339**, 1426-1429, doi:10.1126/science.1229159 (2013).

30 Shibata, T. *et al.* Guanosine and its modified derivatives are endogenous ligands for TLR7. *Int Immunol* **28**, 211-222, doi:10.1093/intimm/dxv062 (2016).

31 Tanji, H. *et al.* Toll-like receptor 8 senses degradation products of single-stranded RNA. *Nat Struct Mol Biol* **22**, 109-115, doi:10.1038/nsmb.2943 (2015).

32 Bell, J. K. *et al.* The molecular structure of the Toll-like receptor 3 ligand-binding domain. *Proc Natl Acad Sci U S A* **102**, 10976-10980, doi:10.1073/pnas.0505077102 (2005).

33 Bell, J. K., Askins, J., Hall, P. R., Davies, D. R. & Segal, D. M. The dsRNA binding site of human Toll-like receptor 3. *Proceedings of the National Academy of Sciences* **103**, 8792, doi:10.1073/pnas.0603245103 (2006).

34 Choe, J., Kelker, M. S. & Wilson, I. A. Crystal structure of human toll-like receptor 3 (TLR3) ectodomain. *Science* **309**, 581-585, doi:10.1126/science.1115253 (2005).

35 Zhong, X. *et al.* The zinc-finger protein ZFYVE1 modulates TLR3-mediated signaling by facilitating TLR3 ligand binding. *Cellular & Molecular Immunology* **17**, 741, doi:10.1038/s41423-019-0265-6 (2020).

36 Yang, Y. *et al.* The RNA-binding protein Mex3B is a coreceptor of Toll-like receptor 3 in innate antiviral response. *Cell Research* **26**, 288, doi:10.1038/cr.2016.16 (2016).

37 Zhu, S., Wang, G., Lei, X. & Flavell, R. A. Mex3B: a coreceptor to present dsRNA to TLR3. *Cell Research* **26**, 391, doi:10.1038/cr.2016.29 (2016).

38 Han, Y. W. *et al.* Distinct dictation of Japanese encephalitis virus-induced neuroinflammation and lethality via triggering TLR3 and TLR4 signal pathways. *PLoS Pathog* **10**, e1004319, doi:10.1371/journal.ppat.1004319 (2014).

39 Iwakiri, D. *et al.* Epstein-Barr virus (EBV)-encoded small RNA is released from EBV-infected cells and activates signaling from Toll-like receptor 3. *J Exp Med* **206**, 2091-

2099, doi:10.1084/jem.20081761 (2009).

40 Lafaille, F. G. *et al.* Impaired intrinsic immunity to HSV-1 in human iPSC-derived TLR3-deficient CNS cells. *Nature* **491**, 769-773, doi:10.1038/nature11583 (2012).

41 Sato, R. *et al.* Combating herpesvirus encephalitis by potentiating a TLR3–mTORC2 axis. *Nature Immunology* **19**, 1071, doi:10.1038/s41590-018-0203-2 (2018).

42 Daffis, S., Samuel, M. A., Suthar, M. S., Gale, M., Jr. & Diamond, M. S. Toll-like receptor 3 has a protective role against West Nile virus infection. *J Virol* **82**, 10349-10358, doi:10.1128/jvi.00935-08 (2008).

43 Kurt-Jones, E. A. *et al.* The role of toll-like receptors in herpes simplex infection in neonates. *J Infect Dis* **191**, 746-748, doi:10.1086/427339 (2005).

44 Wang, T. *et al.* Toll-like receptor 3 mediates West Nile virus entry into the brain causing lethal encephalitis. *Nat Med* **10**, 1366-1373, doi:10.1038/nm1140 (2004).

45 Sancho-Shimizu, V. *et al.* Genetic susceptibility to herpes simplex virus 1 encephalitis in mice and humans. *Curr Opin Allergy Clin Immunol* **7**, 495-505, doi:10.1097/ACI.0b013e3282f151d2 (2007).

46 Zhang, S. Y. *et al.* TLR3 deficiency in patients with herpes simplex encephalitis. *Science* **317**, 1522-1527, doi:10.1126/science.1139522 (2007).

47 Hochrein, H. *et al.* Herpes simplex virus type-1 induces IFN-alpha production via Toll-like receptor 9-dependent and -independent pathways. *Proc Natl Acad Sci U S A* **101**, 11416-11421, doi:10.1073/pnas.0403555101 (2004).

48 Takemura, N. *et al.* Blockade of TLR3 protects mice from lethal radiation-induced gastrointestinal syndrome. *Nat Commun* **5**, 3492, doi:10.1038/ncomms4492 (2014).

49 Ahmad, S. & Hur, S. Helicases in Antiviral Immunity: Dual Properties as Sensors and Effectors. *Trends in Biochemical Sciences* **40**, 576, doi:10.1016/j.tibs.2015.08.001 (2015).

50 Goubau, D., Deddouche, S. & Reis e Sousa, C. Cytosolic sensing of viruses. *Immunity*

38, 855, doi:10.1016/j.immuni.2013.05.007 (2013).

51 Chan, M. P. *et al.* DNase II-dependent DNA digestion is required for DNA sensing by TLR9. *Nat Commun* **6**, 5853, doi:10.1038/ncomms6853 (2015).

52 Abe, T. *et al.* STING recognition of cytoplasmic DNA instigates cellular defense. *Mol Cell* **50**, 5-15, doi:10.1016/j.molcel.2013.01.039 (2013).

53 Ahn, J., Gutman, D., Saijo, S. & Barber, G. N. STING manifests self DNA-dependent inflammatory disease. *Proc Natl Acad Sci U S A* **109**, 19386-19391, doi:10.1073/pnas.1215006109 (2012).

54 Yoshida, H., Okabe, Y., Kawane, K., Fukuyama, H. & Nagata, S. Lethal anemia caused by interferon-beta produced in mouse embryos carrying undigested DNA. *Nat Immunol* **6**, 49-56, doi:10.1038/ni1146 (2005).

55 Crow, Y. J. *et al.* Mutations in the gene encoding the 3'-5' DNA exonuclease TREX1 cause Aicardi-Goutieres syndrome at the AGS1 locus. *Nat Genet* **38**, 917-920, doi:10.1038/ng1845 (2006).

56 Ostendorf, T. *et al.* Immune Sensing of Synthetic, Bacterial, and Protozoan RNA by Toll-like Receptor 8 Requires Coordinated Processing by RNase T2 and RNase 2. *Immunity* **52**, 591, doi:10.1016/j.immuni.2020.03.009 (2020).

57 Becknell, B. *et al.* Ribonucleases 6 and 7 have antimicrobial function in the human and murine urinary tract. *Kidney international* **87**, 151, doi:10.1038/ki.2014.268 (2015).

58 Rademacher, F. *et al.* The Antimicrobial and Immunomodulatory Function of RNase 7 in Skin. *Frontiers in Immunology* **10**, doi:10.3389/fimmu.2019.02553 (2019).

59 Spencer, J. D. *et al.* Ribonuclease 7 is a potent antimicrobial peptide within the human urinary tract. *Kidney International* **80**, 174, doi:10.1038/ki.2011.109 (2011).

60 Campomenosi, P. *et al.* Characterization of RNASET2, the first human member of the Rh/T2/S family of glycoproteins. *Arch Biochem Biophys* **449**, 17-26,

doi:10.1016/j.abb.2006.02.022 (2006).

61 Luhtala, N. & Parker, R. T2 Family ribonucleases: ancient enzymes with diverse roles. *Trends Biochem Sci* **35**, 253-259, doi:10.1016/j.tibs.2010.02.002 (2010).

62 Thompson, D. M. & Parker, R. The RNase Rny1p cleaves tRNAs and promotes cell death during oxidative stress in Saccharomyces cerevisiae. *The Journal of Cell Biology* **185**, 43, doi:10.1083/jcb.200811119 (2009).

63 Haud, N. *et al.* rnaset2 mutant zebrafish model familial cystic leukoencephalopathy and reveal a role for RNase T2 in degrading ribosomal RNA. *Proc Natl Acad Sci U S A* **108**, 1099-1103, doi:10.1073/pnas.1009811107 (2011).

64 Frankel, L. B., Lubas, M. & Lund, A. H. Emerging connections between RNA and autophagy. *Autophagy* **13**, 3, doi:10.1080/15548627.2016.1222992 (2017).

65 Liu, P. *et al.* Mammalian mitochondrial RNAs are degraded in the mitochondrial intermembrane space by RNASET2. *Protein Cell* **8**, 735-749, doi:10.1007/s13238-017-0448-9 (2017).

66 Acquati, F. *et al.* Tumor and metastasis suppression by the human RNASET2 gene. *Int J Oncol* **26**, 1159-1168 (2005).

67 Monti, L. *et al.* RNASET2 as a tumor antagonizing gene in a melanoma cancer model. *Oncol Res* **17**, 69-74 (2008).

68 Henneke, M. *et al.* RNASET2-deficient cystic leukoencephalopathy resembles congenital cytomegalovirus brain infection. *Nat Genet* **41**, 773-775, doi:10.1038/ng.398 (2009).

69 Tonduti, D. *et al.* Clinical, radiological and possible pathological overlap of cystic leukoencephalopathy without megalencephaly and Aicardi-Goutières syndrome. *European Journal of Paediatric Neurology* **20**, 604, doi:10.1016/j.ejpn.2016.03.009 (2016).

70 Sinkevicius, K. W. *et al.* RNaseT2 knockout rats exhibit hippocampal neuropathology

and deficits in memory. *Dis Model Mech* **11**, doi:10.1242/dmm.032631 (2018).

71 Hamilton, N. *et al.* The failure of microglia to digest developmental apoptotic cells contributes to the pathology of RNASET2-deficient leukoencephalopathy. *Glia* **68**, 1531, doi:10.1002/glia.23829 (2020).

72 Greulich, W. *et al.* TLR8 Is a Sensor of RNase T2 Degradation Products. *Cell* **179**, 1264, doi:10.1016/j.cell.2019.11.001 (2019).

73 Weber, T. *et al.* Zebrafish disease model of human RNASET2-deficient cystic leukoencephalopathy displays abnormalities in early microglia. *Biology Open* **9**, doi:10.1242/bio.049239 (2020).

74 Saitoh, S.-I. *et al.* TLR7 mediated viral recognition results in focal type I interferon secretion by dendritic cells. *Nature Communications* **8**, doi:10.1038/s41467-017-01687-x (2017).

75 Murakami, Y. *et al.* Roles of the Cleaved N-Terminal TLR3 Fragment and Cell Surface TLR3 in Double-Stranded RNA Sensing. *The Journal of Immunology* **193**, 5208, doi:10.4049/jimmunol.1400386 (2014).

76 Parry, S., Newbigin, E., Currie, G., Bacic, A. & Oxley, D. Identification of active-site histidine residues of a self-incompatibility ribonuclease from a wild tomato. *Plant Physiology* **115**, 1421, doi:10.1104/pp.115.4.1421 (1997).

77 Nishikawa, S. *et al.* Two histidine residues are essential for ribonuclease T1 activity as is the case for ribonuclease A. *Biochemistry* **26**, 8620, doi:10.1021/bi00400a019 (1987).

78 Vidalino, L. *et al.* Intracellular trafficking of RNASET2, a novel component of P-bodies. *Biol Cell* **104**, 13-21, doi:10.1111/boc.201100092 (2012).

79 Sato, R. *et al.* The impact of cell maturation and tissue microenvironments on the expression of endosomal Toll-like receptors in monocytes and macrophages. *International Immunology* **32**, 785, doi:10.1093/intimm/dxaa055 (2020).

80 Nguyen, T. A. *et al.* SIDT2 Transports Extracellular dsRNA into the Cytoplasm for Innate Immune Recognition. *Immunity* **47**, 498, doi:10.1016/j.immuni.2017.08.007 (2017).

81 Chiappinelli, Katherine B. *et al.* Inhibiting DNA Methylation Causes an Interferon Response in Cancer via dsRNA Including Endogenous Retroviruses. *Cell* **162**, 974, doi:10.1016/j.cell.2015.07.011 (2015).

82 Liddicoat, B. J. *et al.* RNA editing by ADAR1 prevents MDA5 sensing of endogenous dsRNA as nonself. *Science* **349**, 1115, doi:10.1126/science.aac7049 (2015).